SAND2019-6283C

Multiscale Modeling of Microstructure and Performance in Additively Manufactured Parts

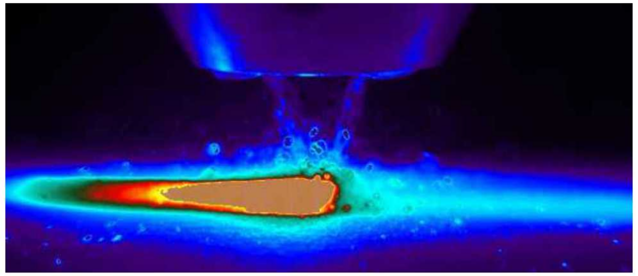

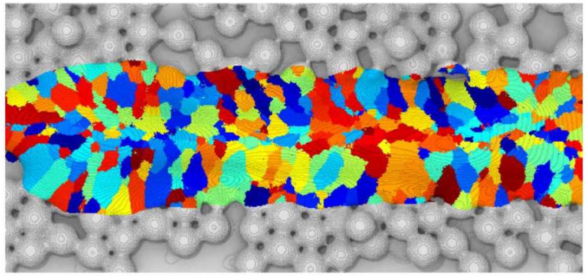

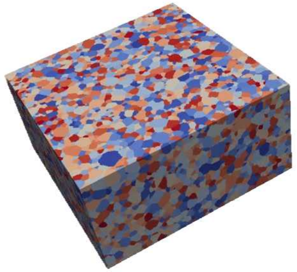

PRESENTED BY

Kyle Johnson, Theron Rodgers, John Emery, Joe Bishop, Kyle Karlson, Mike Stender, Guy Bergel, Bradley Jared, Chris Hammetter, Spencer Grange, Kurtis Ford, and Judy Brown

Sandia National Laboratories is a multimission laboratory managed and operated by National Technology & Engineering Solutions of Sandia, LLC, a wholly owned subsidiary of Honeywell International Inc., for the U.S. Department of Energy's National Nuclear Security Administration under contract DE-NA0003525.

Long-Term Vision for AM Adoption

Taken from Born Qualified Grand Challenge LDRD: Revolutionize design and manufacturing by combining Additive Manufacturing (AM) techniques with deep materials and process understanding to transform qualification paradigms where materials, designs, and ultimately components are *Born Qualified*

- ➢ Inherently requires linking Process-Structure-Property-Performance (PSPP)* relationships

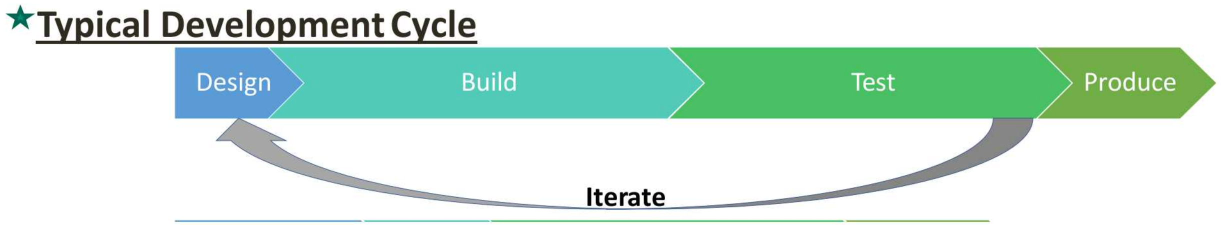

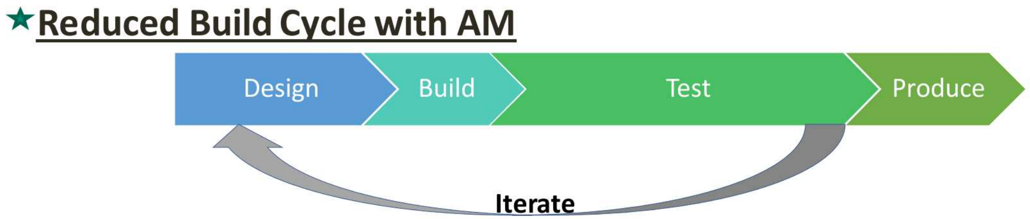

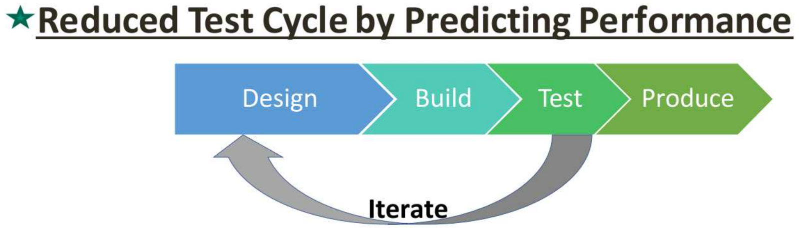

+ Agility = rapid response to emerging challenges
+ Faster failures & successes
+ More build iterations = greater confidence
+ More time to design
+ Cost & schedule savings

Figure: Allen Roach

* Olson *Science*, 2000

Models Bridging Length Scales

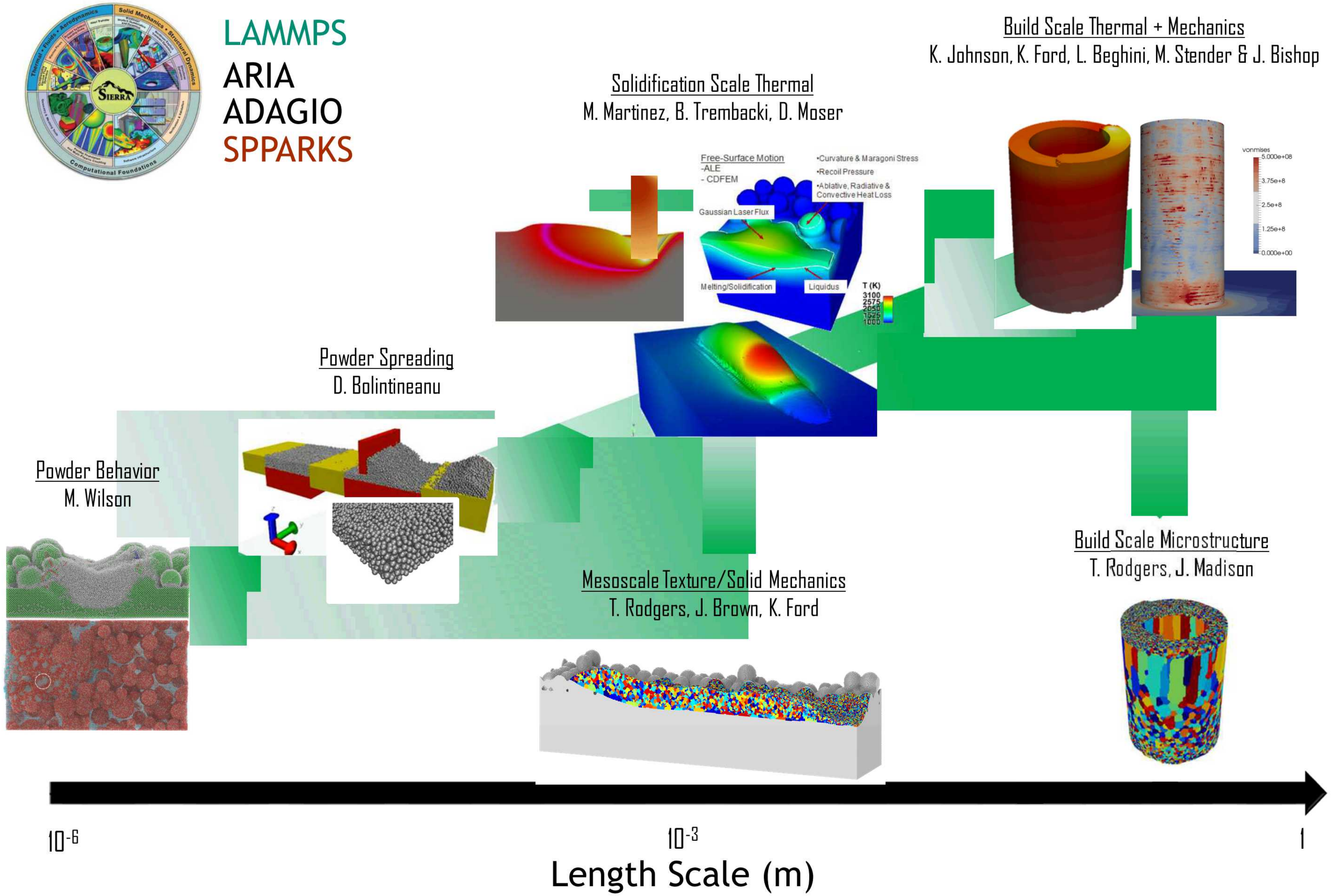

Progress Toward Linking Process-Structure-Property-Performance Relationships

1. Residual Stress Prediction at Varying Fidelity and Efficiency

2. Microstructure Prediction

3. Predicting the Mechanical Performance and Failure of As-Built Parts

High Fidelity Process Models Provide Resolution at Each Laser Pass

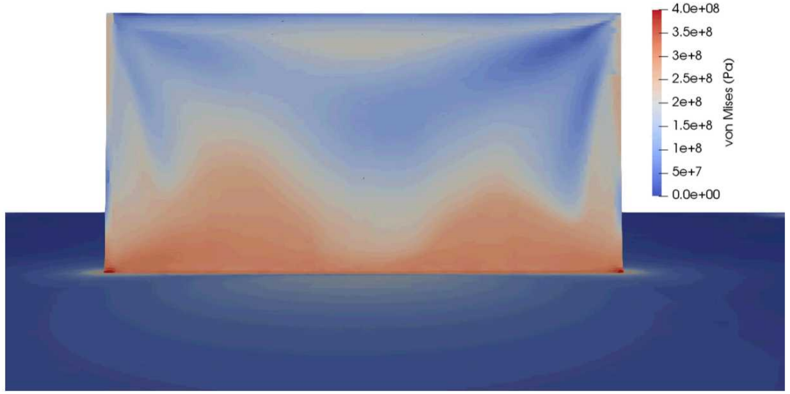

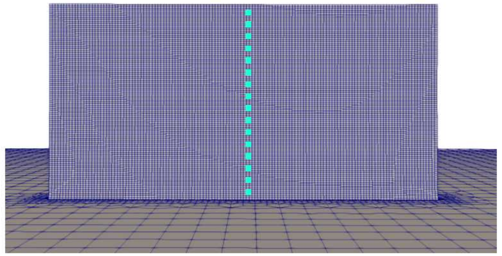

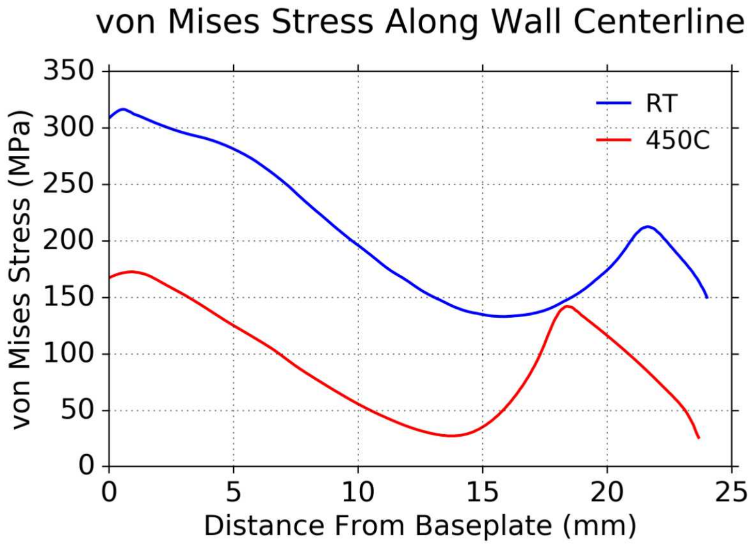

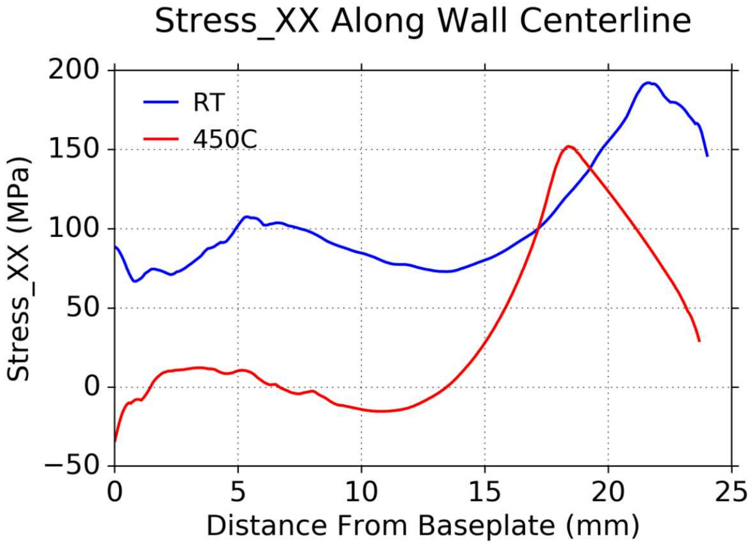

304L Two Pass LENS Thin Wall Build Study Examining Baseplate Preheating Effects

High Fidelity Models Inform Reduced Order Models

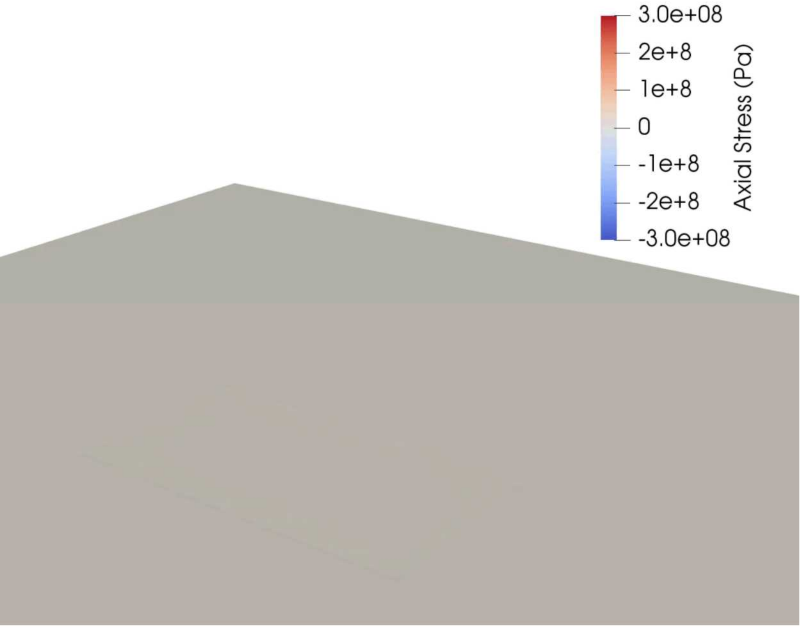

Enlarged Heat Source* and Layer Thickness
100 cpus
6 hrs (~real time)

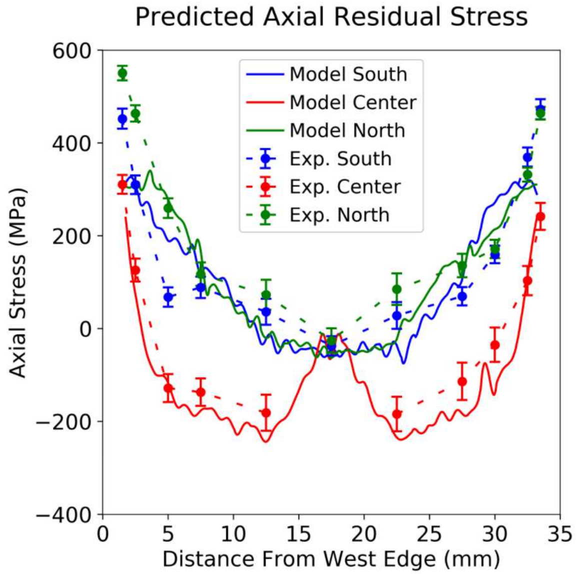

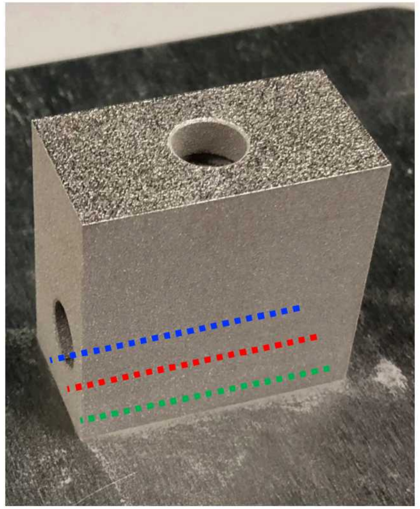

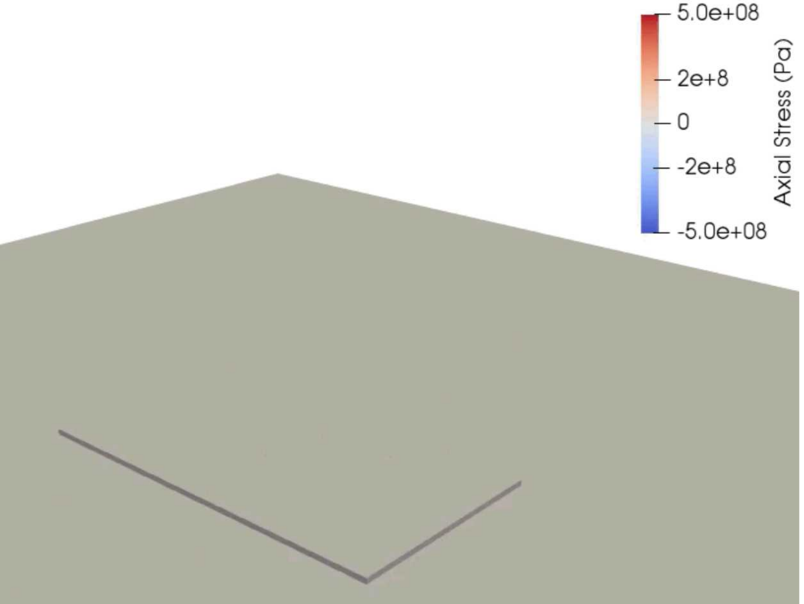

Mechanical Inherent Strain
60 cpus
30 minutes

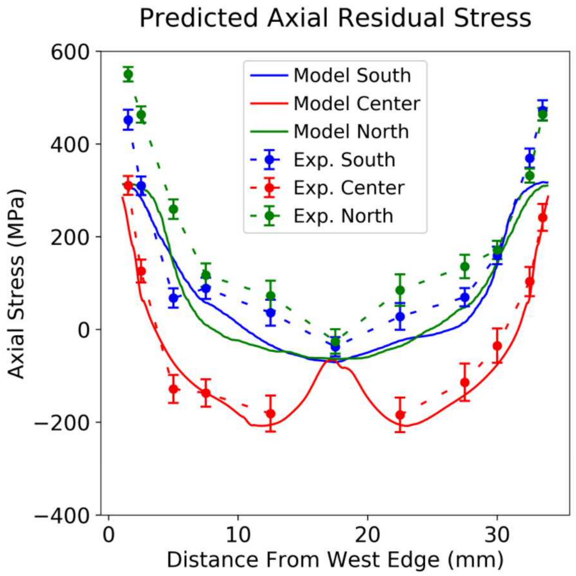

* Similar to Hodge et al. 2014 and 2016, Ganeriwala et al. 2019

Progress Toward Linking Process-Structure-Property-Performance Relationships

1. Residual Stress Prediction at Varying Fidelity and Efficiency

2. Microstructure Prediction

3. Predicting the Mechanical Performance and Failure of As-Built Parts

Microstructure Prediction in Stochastic Parallel PARticle Kinetic Simulator (SPPARKS) - http://spparks.sandia.gov

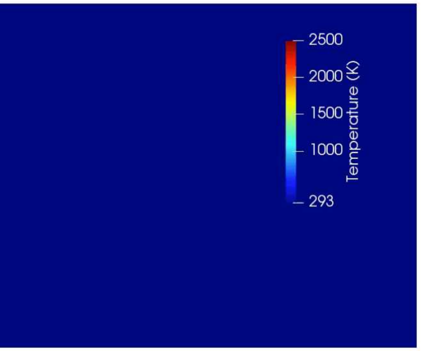

Thermal Simulation from Sierra/Aria (Thermal/Fluid Solver)

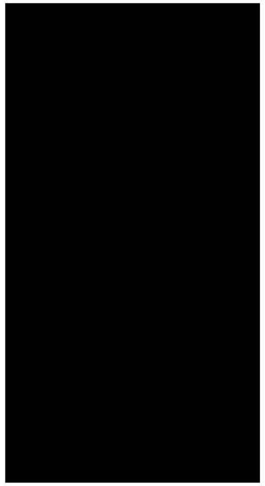

Single Continuous Build

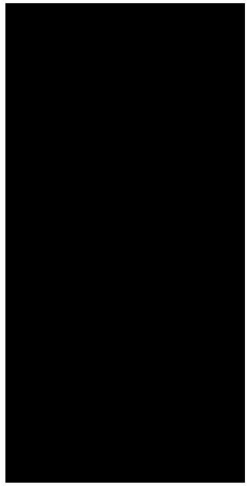

Double Build (8 second delay in between layers)

304L Tube, Johnson et al. *Computational Mechanics* 2018

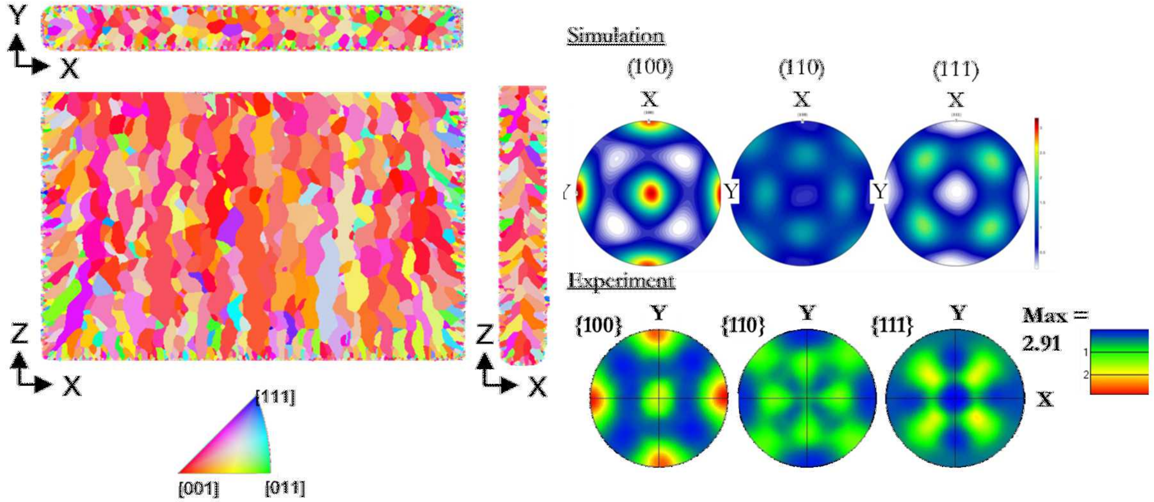

Stainless Steel Thin Wall Texture Prediction

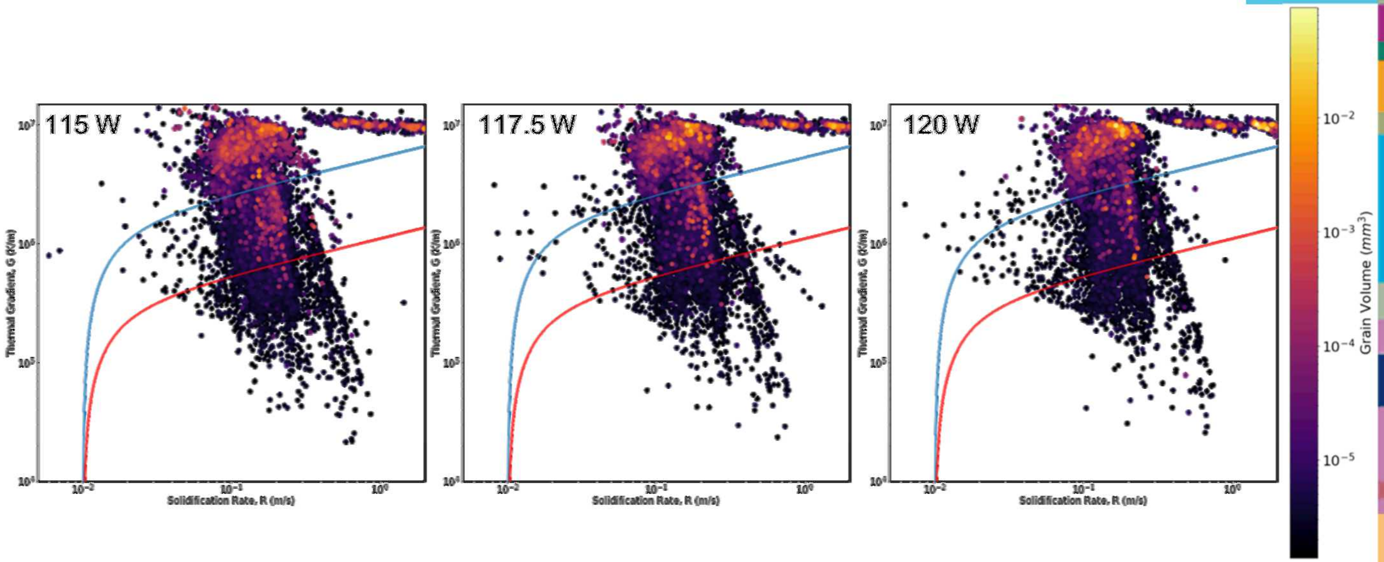

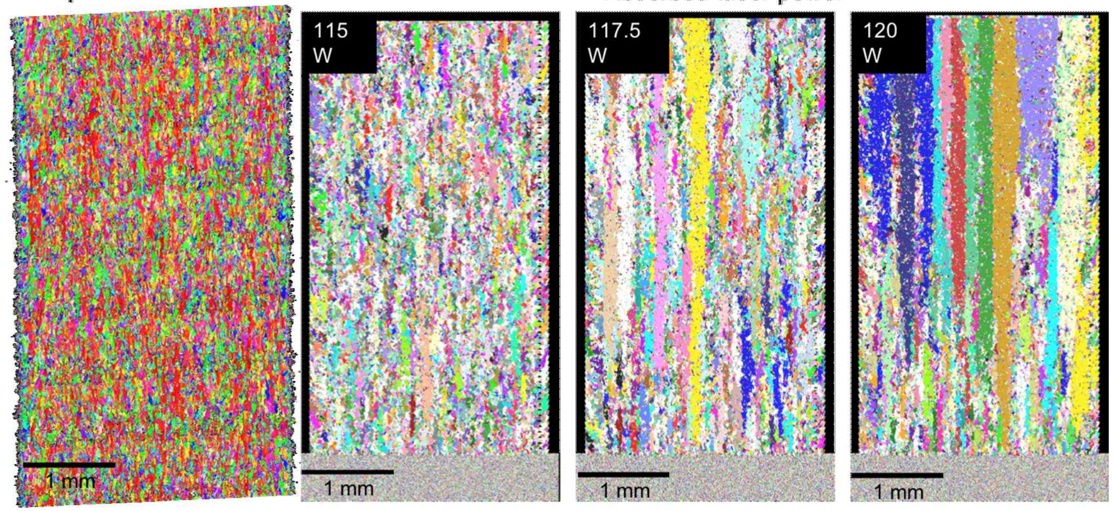

All simulations performed with nucleation densities of 8e13

316L Stainless Steel Column

T. Rodgers, M. Martinez, D. Moser

Progress Toward Linking Process-Structure-Property-Performance Relationships

1. Residual Stress Prediction at Varying Fidelity and Efficiency

2. Microstructure Prediction

3. Predicting the Mechanical Performance and Failure of As-Built Parts

Sandia Fracture Challenge: Blind Predictions of Ductile Failure

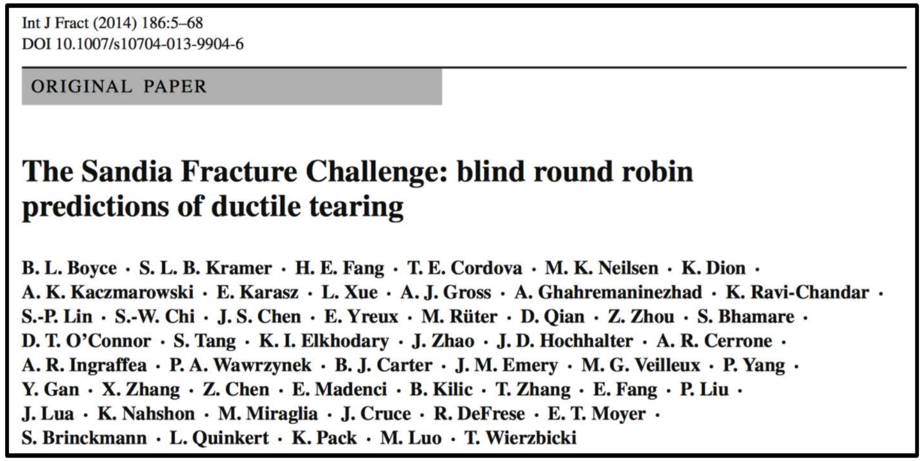

Int J Fract (2014) 186:5–68
DOI 10.1007/s10704-013-9904-6

ORIGINAL PAPER

The Sandia Fracture Challenge: blind round robin predictions of ductile tearing

B. L. Boyce · S. L. B. Kramer · H. E. Fang · T. E. Cordova · M. K. Neilsen · K. Dion · A. K. Kaczmarowski · E. Karasz · L. Xue · A. J. Gross · A. Ghahremaninezhad · K. Ravi-Chandar · S.-P. Lin · S.-W. Chi · J. S. Chen · E. Yreux · M. Rüter · D. Qian · Z. Zhou · S. Bhamare · D. T. O'Connor · S. Tang · K. I. Elkhodary · J. Zhao · J. D. Hochhalter · A. R. Cerrone · A. R. Ingraffea · P. A. Wawrzynek · B. J. Carter · J. M. Emery · M. G. Veilleux · P. Yang · Y. Gan · X. Zhang · Z. Chen · E. Madenci · B. Kilic · T. Zhang · E. Fang · P. Liu · J. Lua · K. Nahshon · M. Miraglia · J. Cruce · R. DeFrese · E. T. Moyer · S. Brinckmann · L. Quinkert · K. Pack · M. Luo · T. Wierzbicki

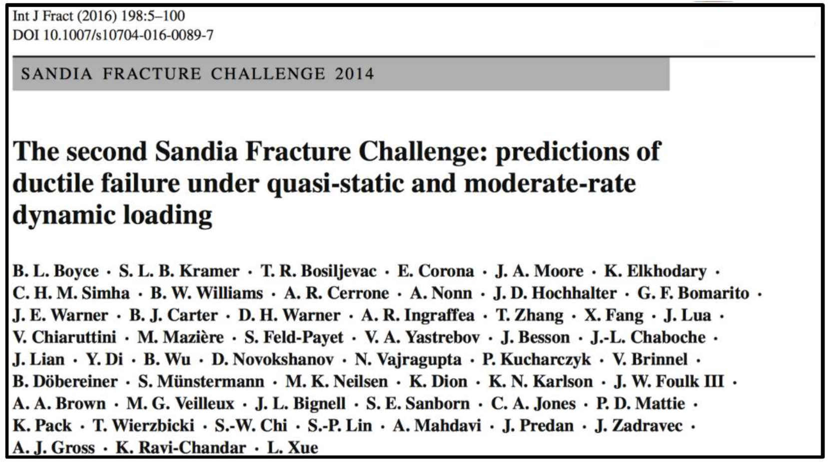

Int J Fract (2016) 198:5–100
DOI 10.1007/s10704-016-0089-7

SANDIA FRACTURE CHALLENGE 2014

The second Sandia Fracture Challenge: predictions of ductile failure under quasi-static and moderate-rate dynamic loading

B. L. Boyce · S. L. B. Kramer · T. R. Bosiljevac · E. Corona · J. A. Moore · K. Elkhodary · C. H. M. Simha · B. W. Williams · A. R. Cerrone · A. Nonn · J. D. Hochhalter · G. F. Bomarito · J. E. Warner · B. J. Carter · D. H. Warner · A. R. Ingraffea · T. Zhang · X. Fang · J. Lua · V. Chiaruttini · M. Mazière · S. Feld-Payet · V. A. Yastrebov · J. Besson · J.-L. Chaboche · J. Lian · Y. Di · B. Wu · D. Novokshanov · N. Vajragupta · P. Kucharczyk · V. Brinnel · B. Döbereiner · S. Münstermann · M. K. Neilsen · K. Dion · K. N. Karlson · J. W. Foulk III · A. A. Brown · M. G. Veilleux · J. L. Bignell · S. E. Sanborn · C. A. Jones · P. D. Mattie · K. Pack · T. Wierzbicki · S.-W. Chi · S.-P. Lin · A. Mahdavi · J. Predan · J. Zadravec · A. J. Gross · K. Ravi-Chandar · L. Xue

The Third Sandia Fracture Challenge – 2016

- 316L AM Part
- Goal: Predict Tensile Failure
- 21 Participant Teams

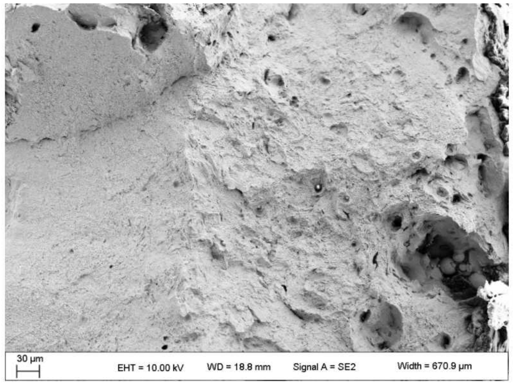

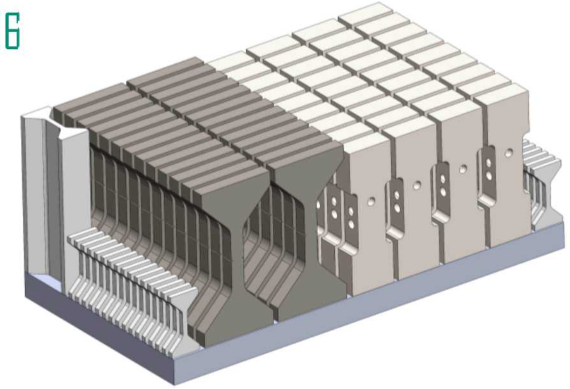

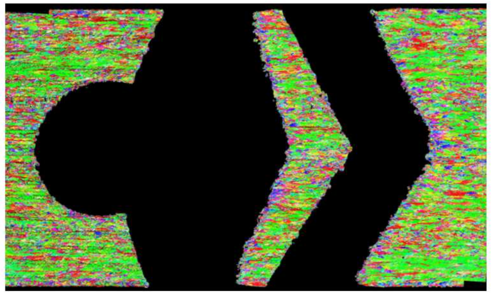

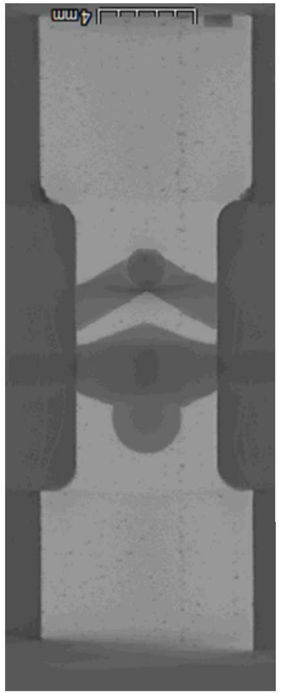

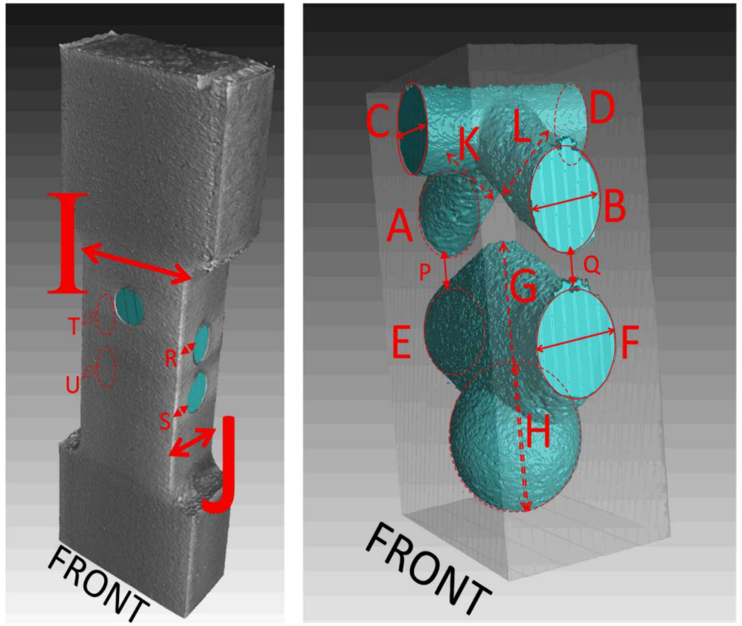

Bammann-Chiesa-Johnson (BCJ) Constitutive Model for Plasticity

- Based on work by Bammann et al. 1993, Brown and Bammann 2012
- History-dependent viscoplastic internal state variable model
- Stress is dependent on damage ϕ and evolves according to

$$\dot{\sigma}_{ij} = \left(\frac{\dot{E}}{E} - \frac{\dot{\phi}}{1-\phi}\right)\sigma_{ij} + E(1-\phi)\left(\dot{\epsilon}_{ij} - \dot{\epsilon}_{ij}^{p}\right)$$

- Flow rule includes yield stress and internal state variable for hardening

$$\dot{\epsilon}_p = \sinh\langle\frac{\sigma_e}{Y+\kappa} - 1\rangle$$

- The isotropic hardening variable κ evolves in a hardening minus recovery form.

$$\dot{\kappa} = \kappa\frac{\dot{\mu}}{\mu} + (H - R_d\kappa)\dot{\epsilon}_p$$

Johnson et al. IJF (Accepted)

Fracture Surfaces Indicated Both Existing Pores and Pore Nucleation

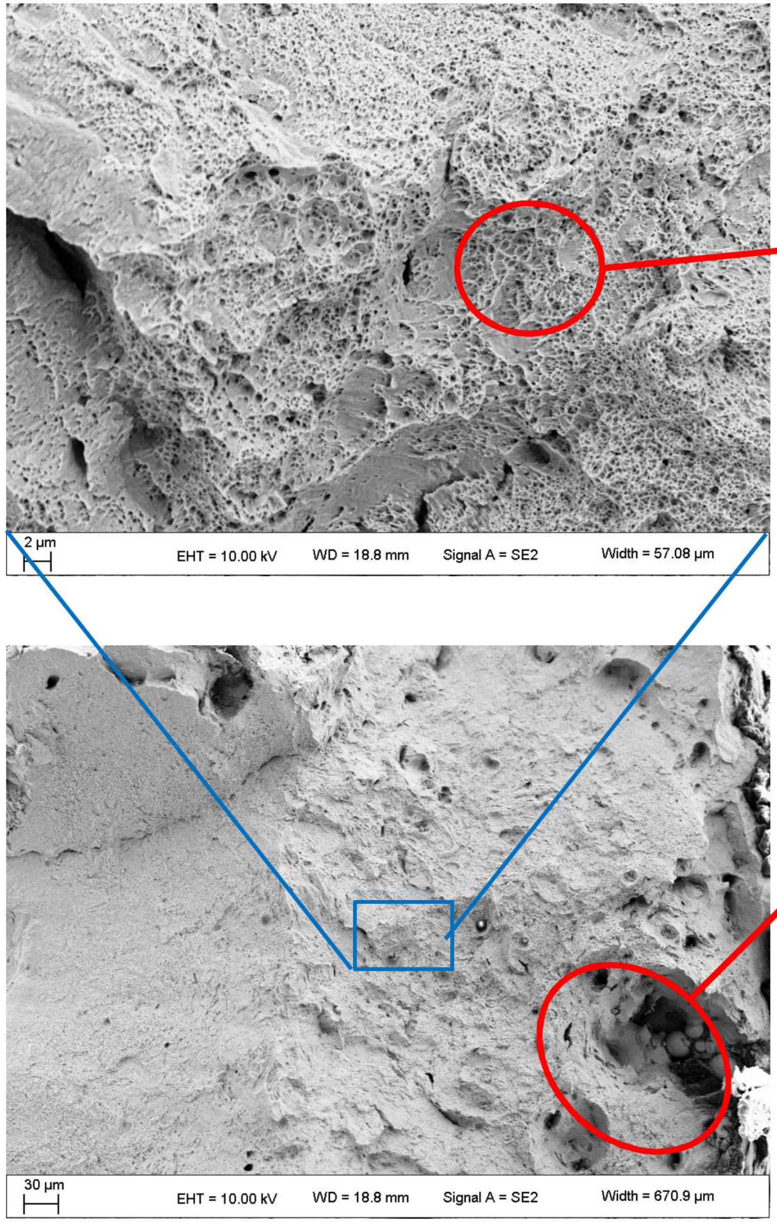

Void Nucleation

Fine scale voids (< 1μm) indicate nucleation

$$\dot{\eta} = \eta \dot{\epsilon}_p \left(N_1 \left[\frac{4}{27} - \frac{J_3^2}{J_2^3} \right] + N_2 \frac{J_3}{J_2^3} + N_3 \frac{\langle p \rangle}{\sigma_e} \right)$$

Void Growth

Pre-existing voids captured by void growth

$$\dot{\phi} = \sqrt{\frac{2}{3}} \dot{\epsilon}_p \frac{1 - (1-\phi)^{m+1}}{(1-\phi)^m} \sinh \left[\frac{2\,(2m-1)}{2m+1} \frac{\langle p \rangle}{\sigma_e} \right]$$

Total Damage

$$\phi = \frac{\eta v_v}{1 + \eta v_v}$$

(Horstemeyer & Gokhale 1999)

Johnson et al. IJF (Accepted)

Incorporating Porosity as Initial Damage

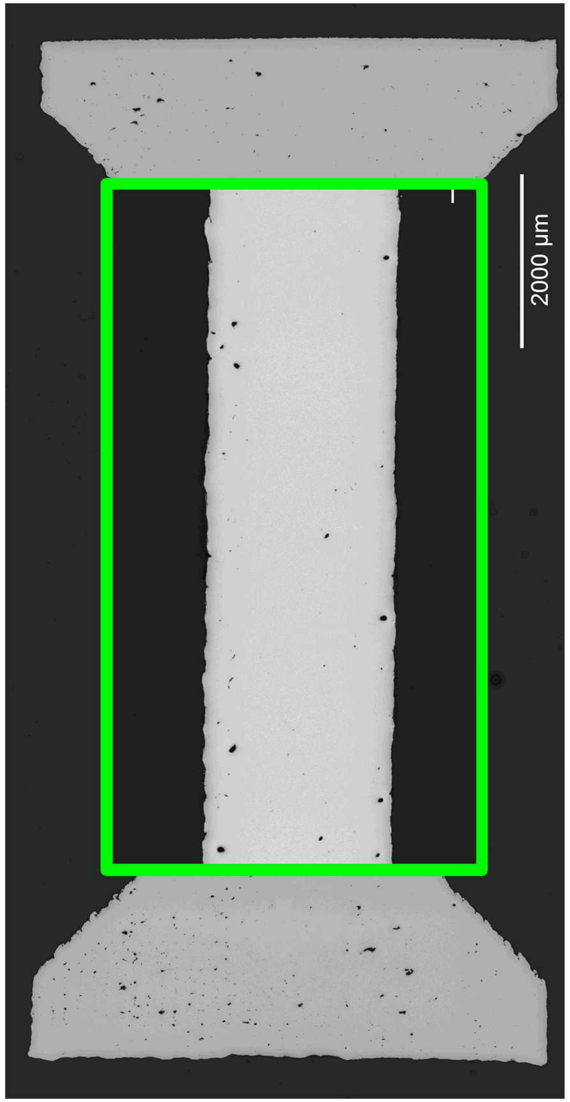

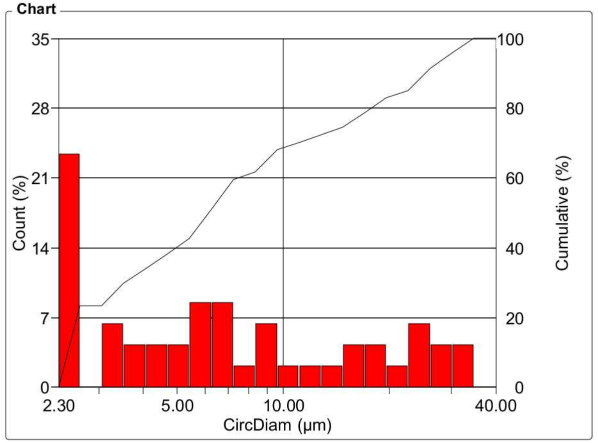

Porosity Mapping

x,y,z,r_{pore}

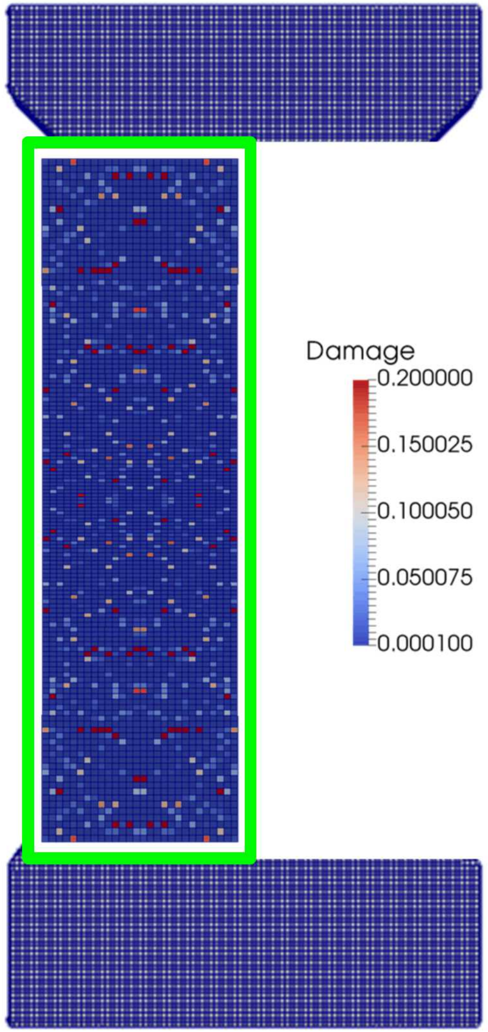

Johnson et al. IJF (Accepted)

Calibration Results for High Throughput Tensile Testing

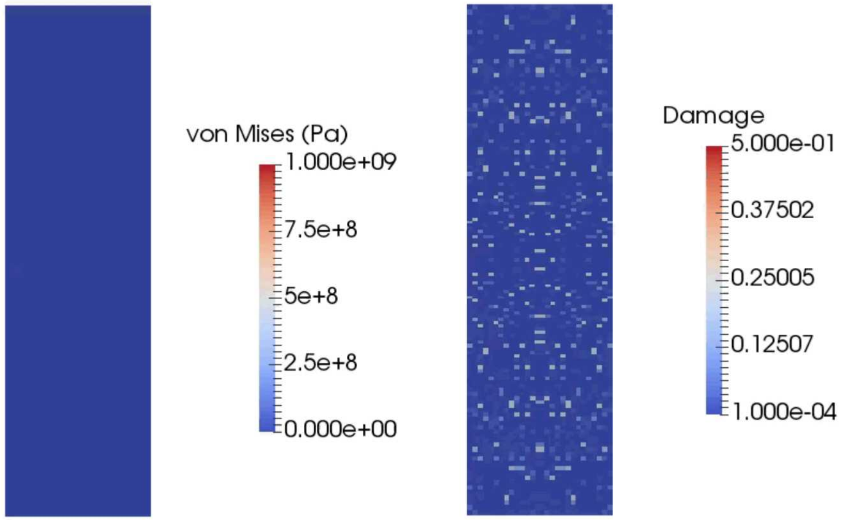

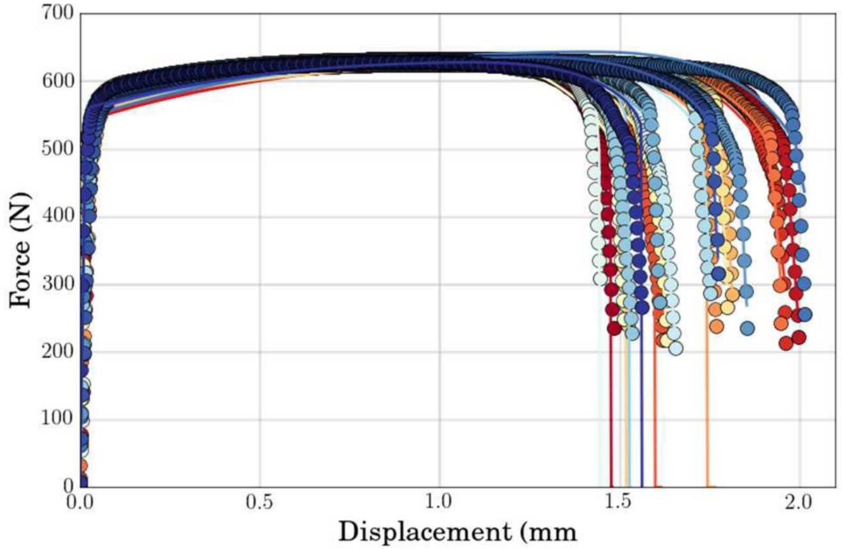

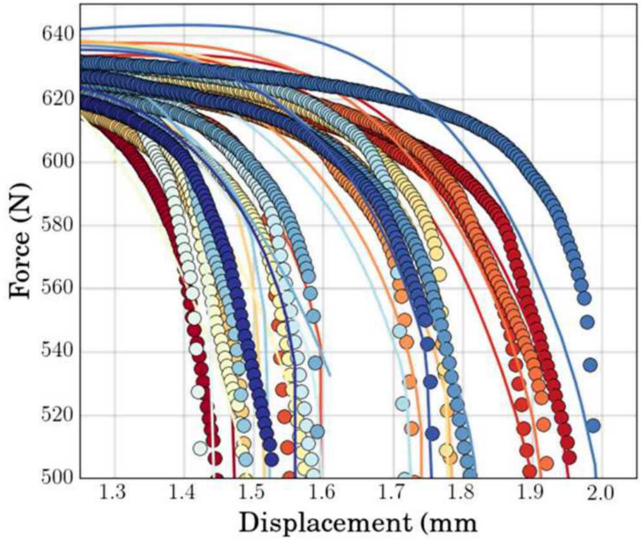

- A parameter set was calibrated for each longitudinal tension test
- Transverse and notched tensile data were not used due to time constraints
- FEA performed in Sierra/SM
- Calibration performed using Dakota and MatCal (Kyle Karlson)

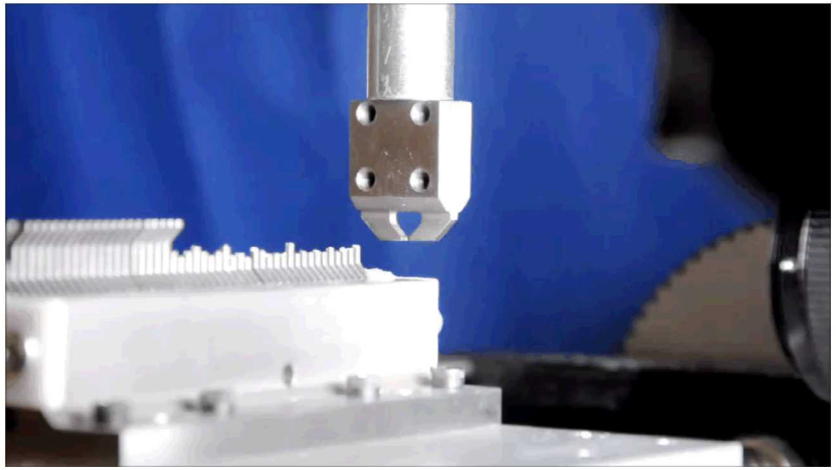

Boyce et al., Adv Eng Mat 2017, Salzbrenner et al. JMPT 2017

Johnson et al. IJF (Accepted)

Porosity Overlaid on Quarter-Symmetry Challenge Geometry

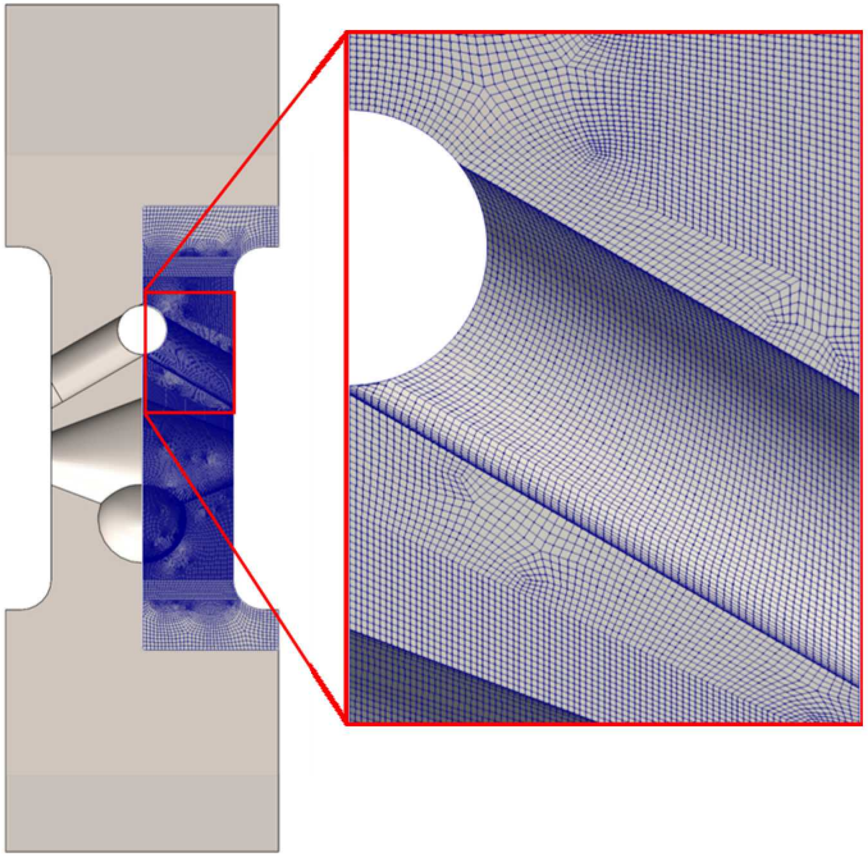

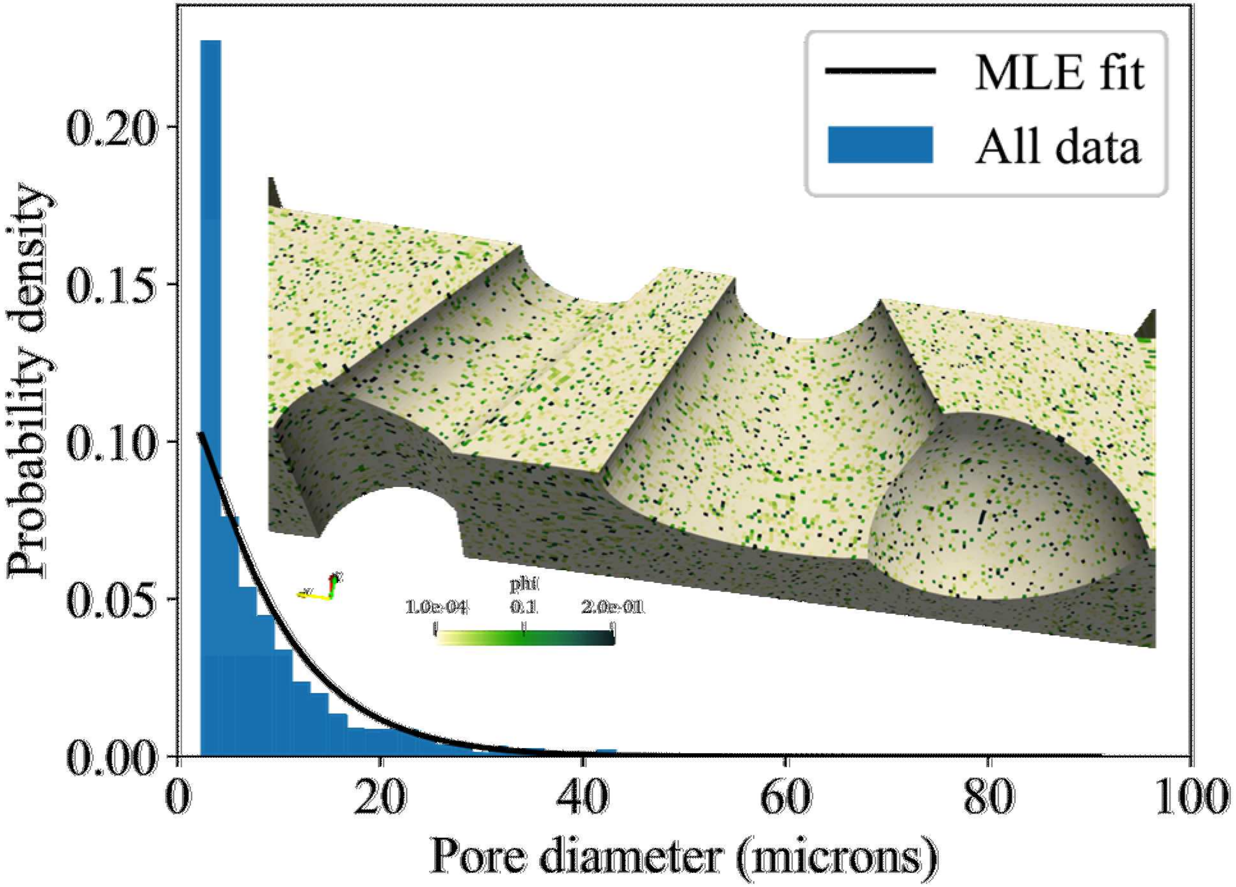

- Multiple porosity initializations were used to capture uncertainty in performance

Johnson et al. IJF (Accepted)

Blind Performance Prediction

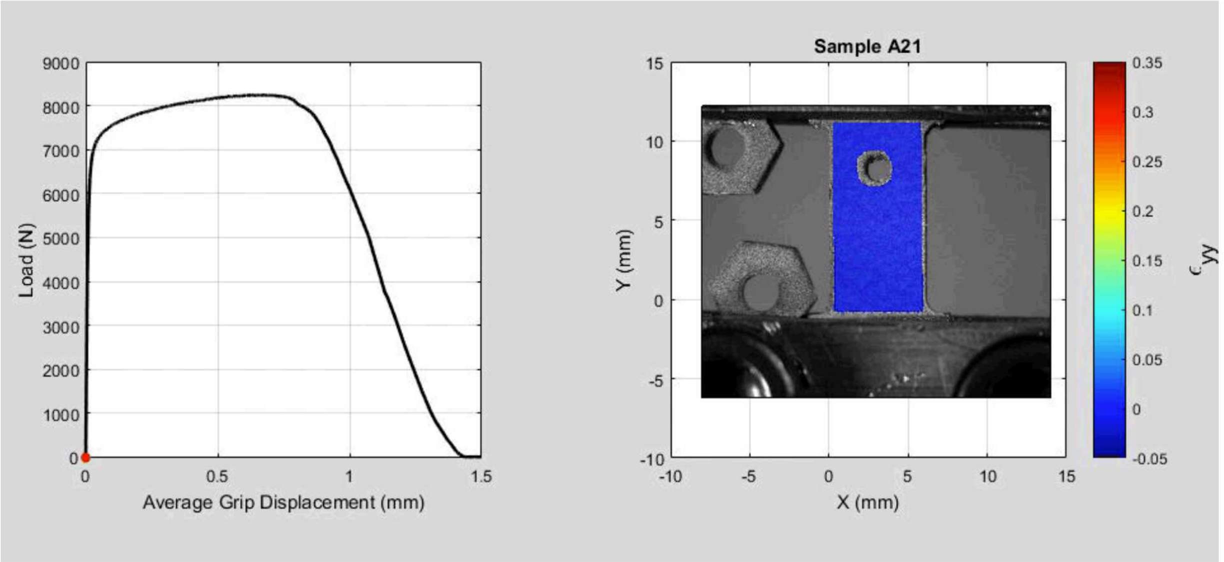

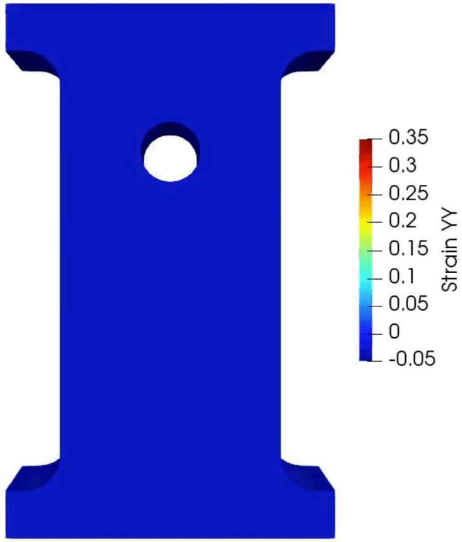

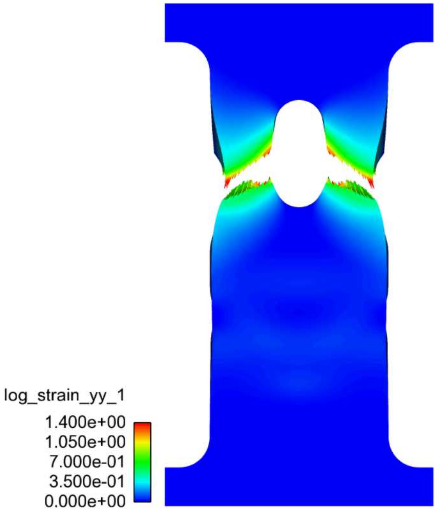

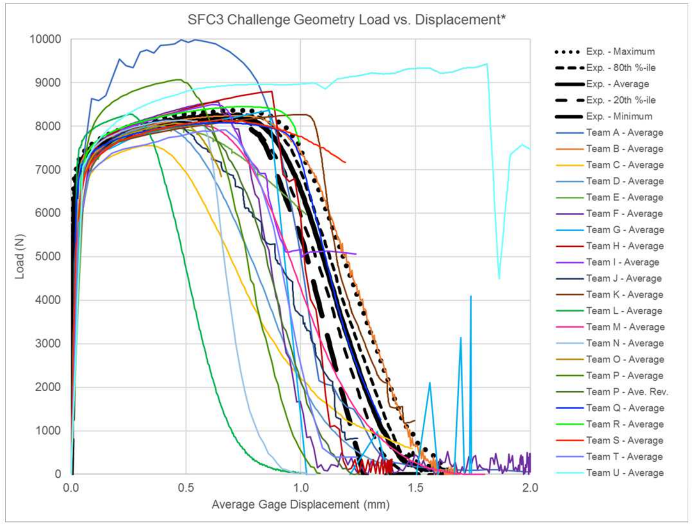

All Participant Predictions with Experimental in Black

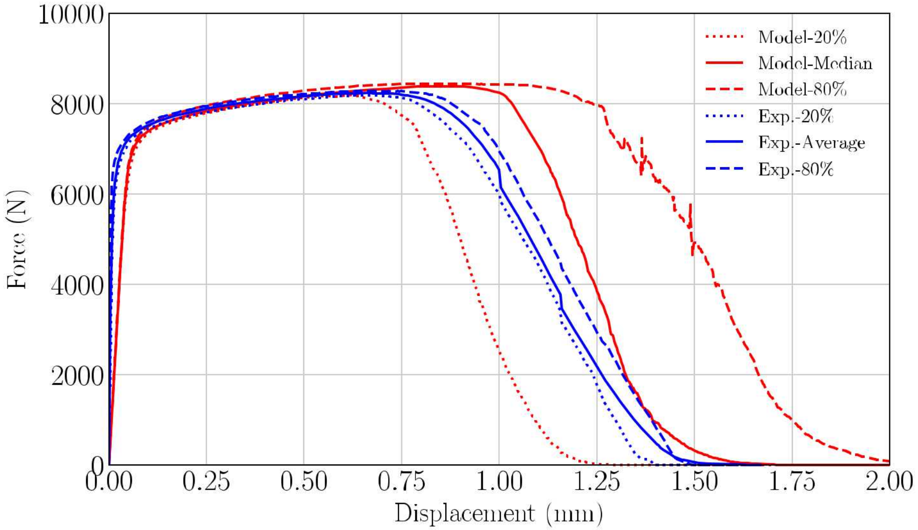

SNL/NM Prediction

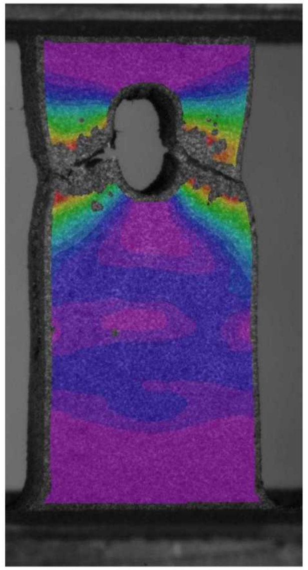

Johnson et al. IJF (Accepted), Kramer, Boyce et al., IJF (Accepted)

Different Porosity Distributions Affect Crack Path

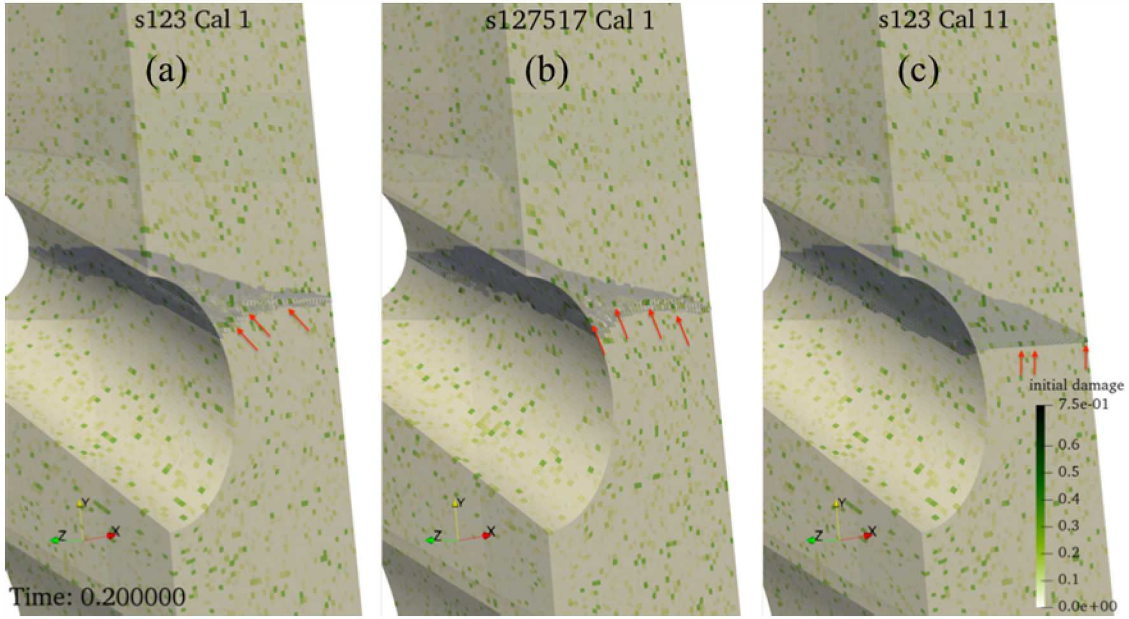

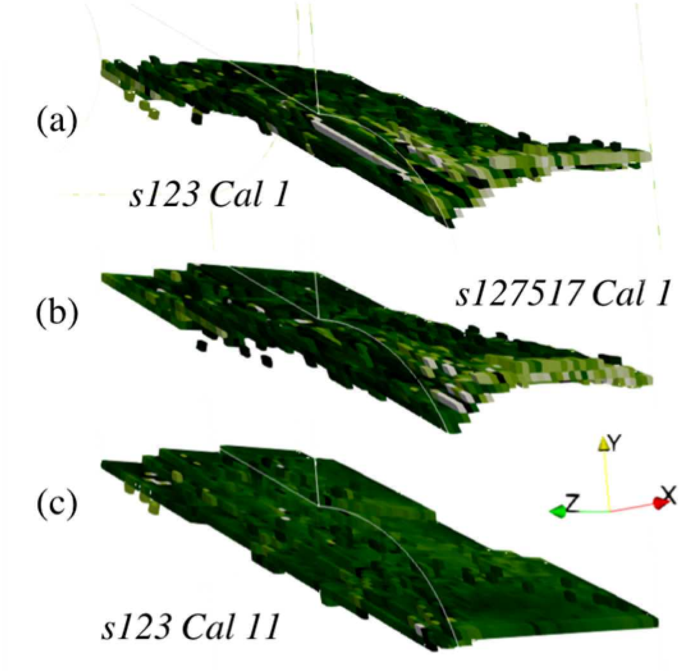

- Porosity seed indicated by *s* number, i.e. s123 is a different realization than s127517
- For the same calibration number (Cal 1), a different porosity seed yields a different crack path

Johnson et al. IJF (Accepted)

Modeling the Effect of Pores and Surface Roughness From High-Resolution CT Scan in Follow-up Investigation

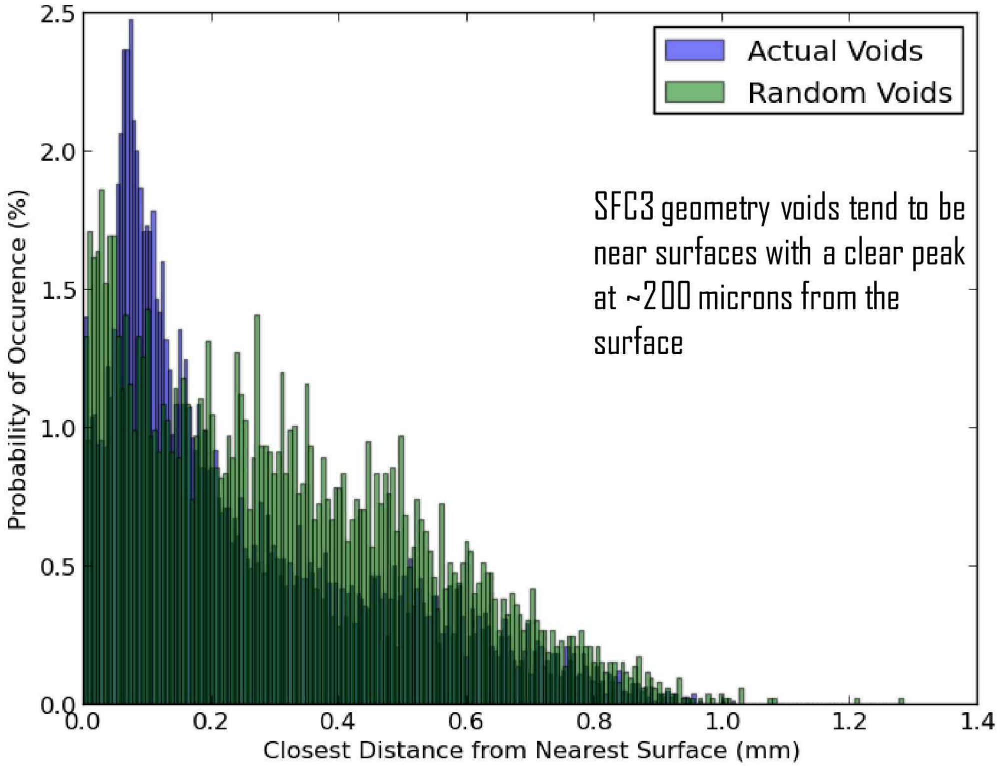

SFC3 geometry voids tend to be near surfaces with a clear peak at ~200 microns from the surface

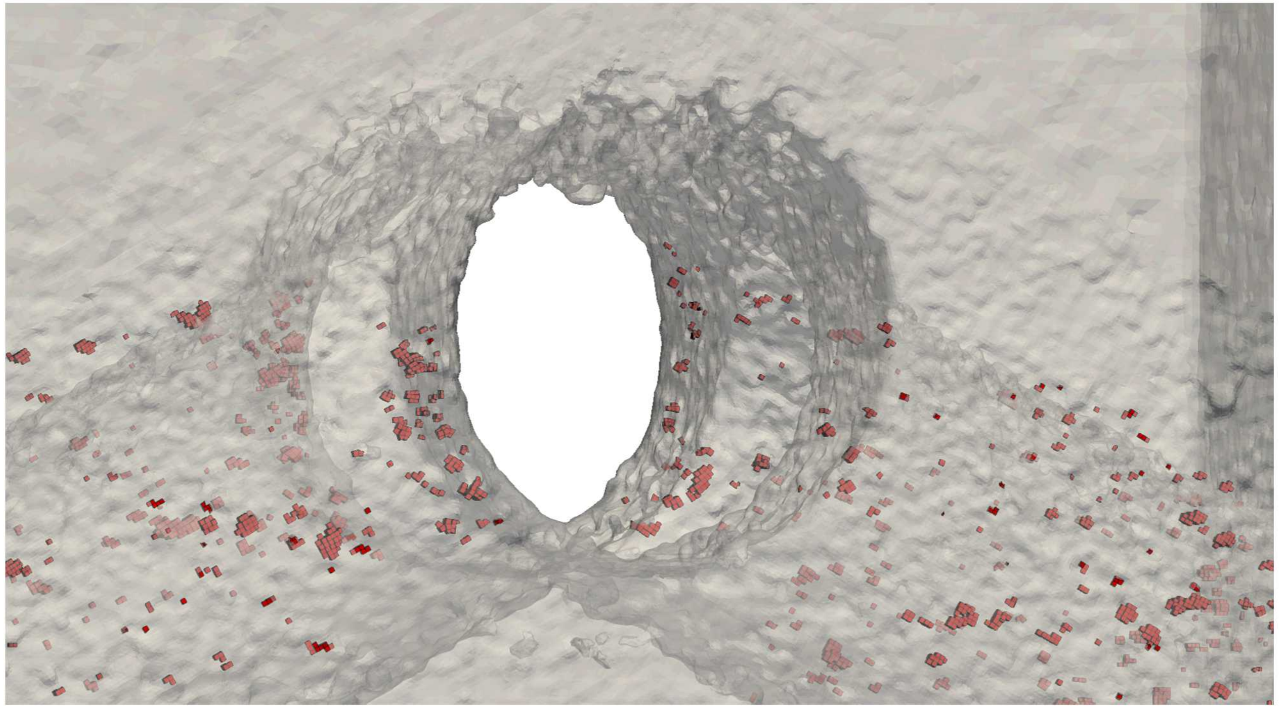

Goal: Develop stochastic relationships for void locations based on relevant parameters such as void clustering, void distance from free surfaces and void volume fraction and apply to porosity overlay approach in efficient models

Slide Courtesy: Kyle Karlson, Guy Bergel

Inclusion of Voids and Roughness Changes Material Response

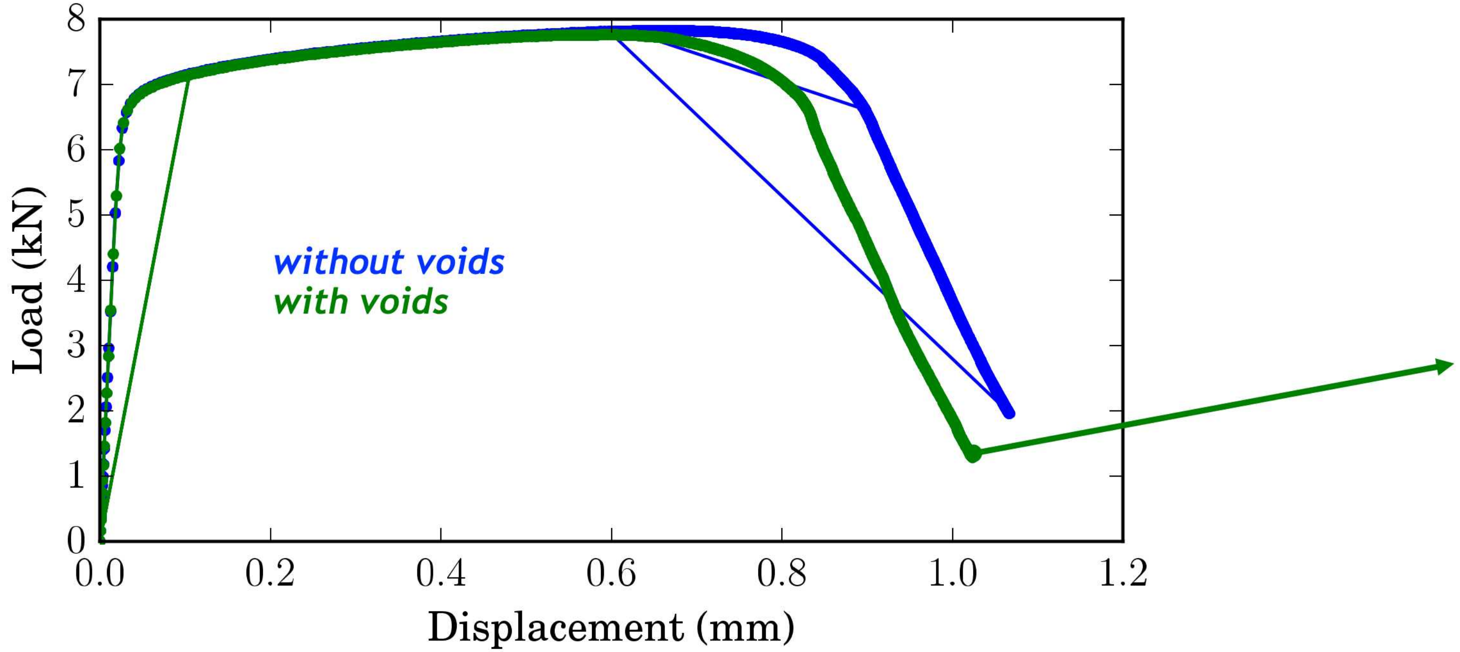

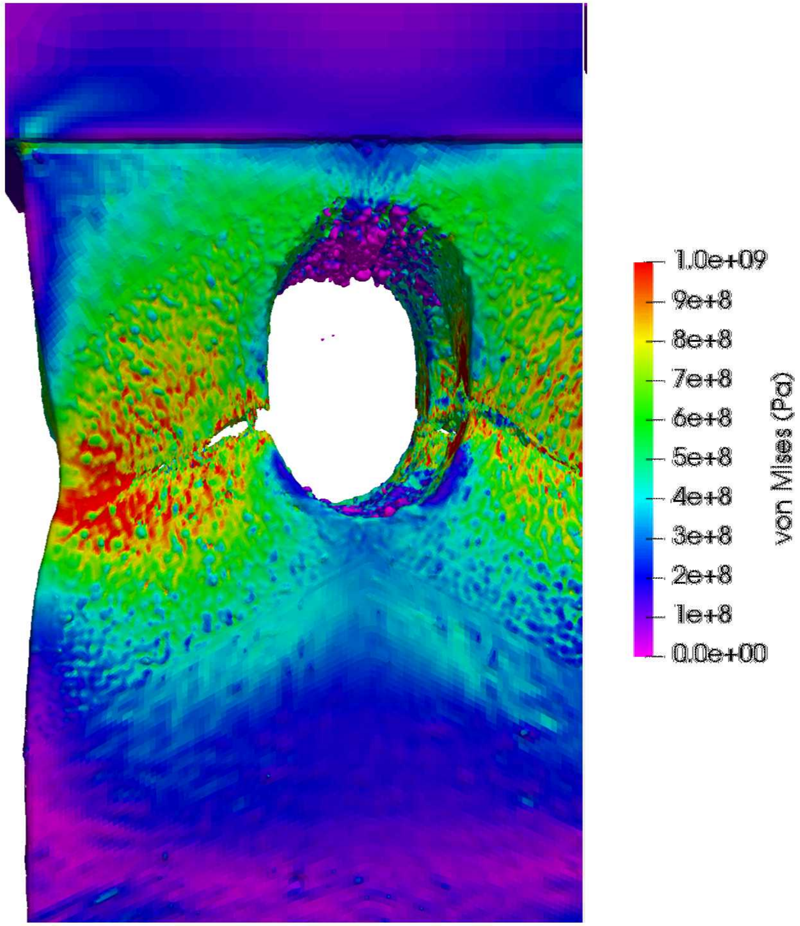

Simulation results from ~13 million element meshes generated from CT scans.

Slide Courtesy: Kyle Karlson, Guy Bergel

Failure Prediction Goal

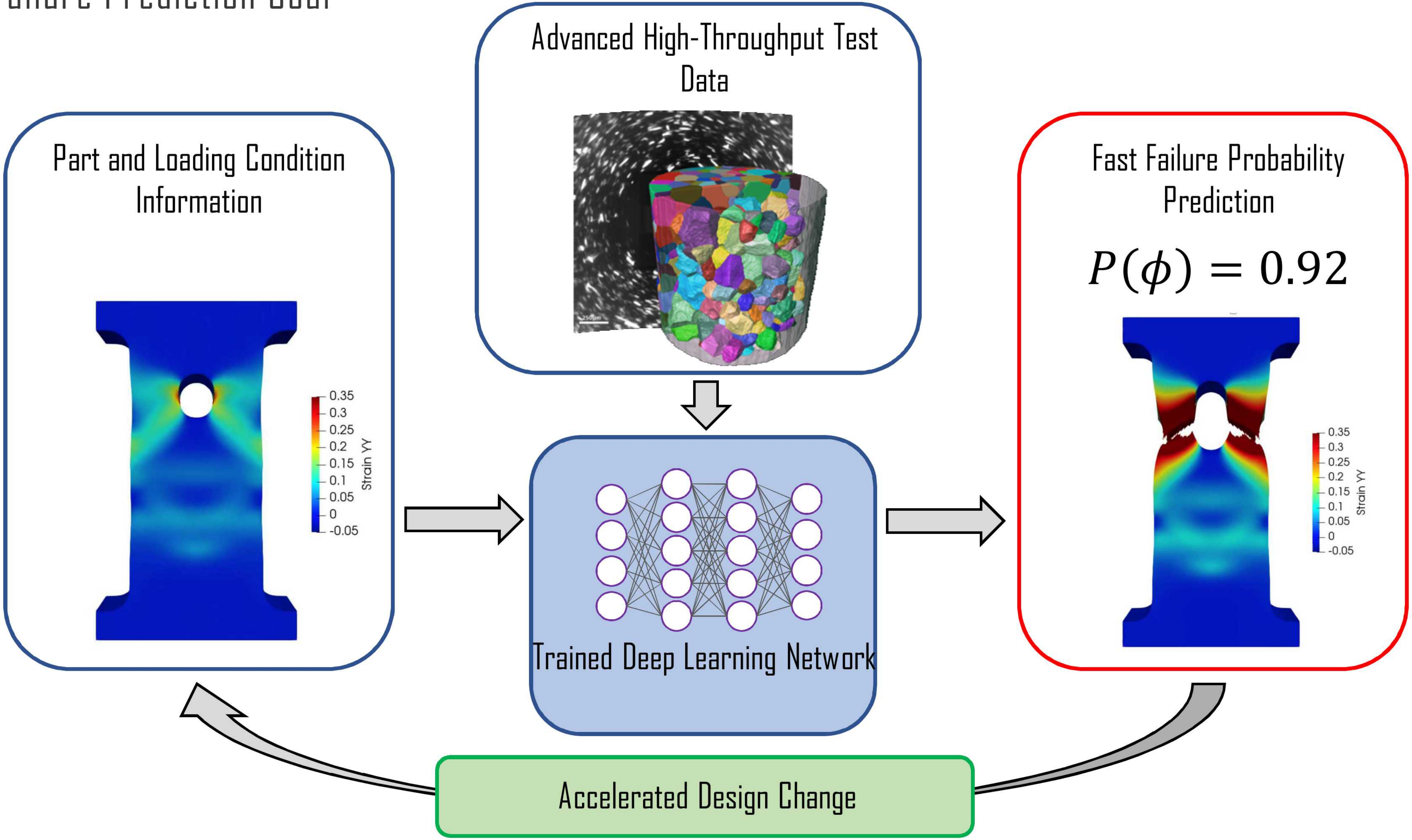

A Tribute to Tarek Zohdi: *A Posteriori* Error-Estimation Techniques Offer Path to Efficiently Represent AM Microstructure When Scale Separation Fails

1. Generate Microstructures Using Kinetic Monte Carlo (KMC)

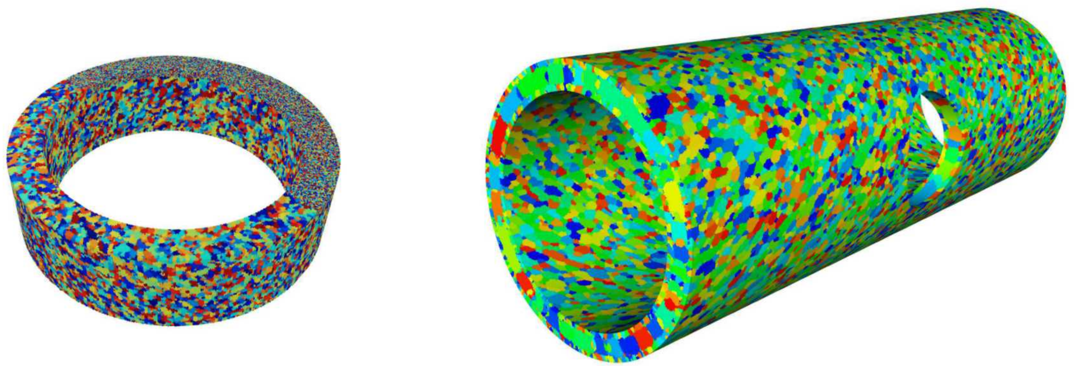

2. Run Homogenous Simulation With Isotropic Material Model

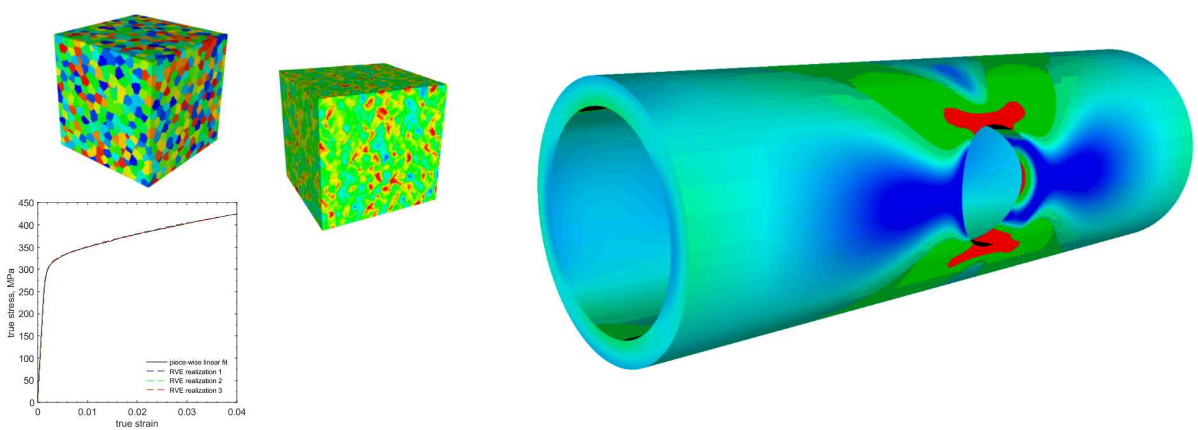

3. Recover Localized Stresses Using *a posteriori* Error Methods

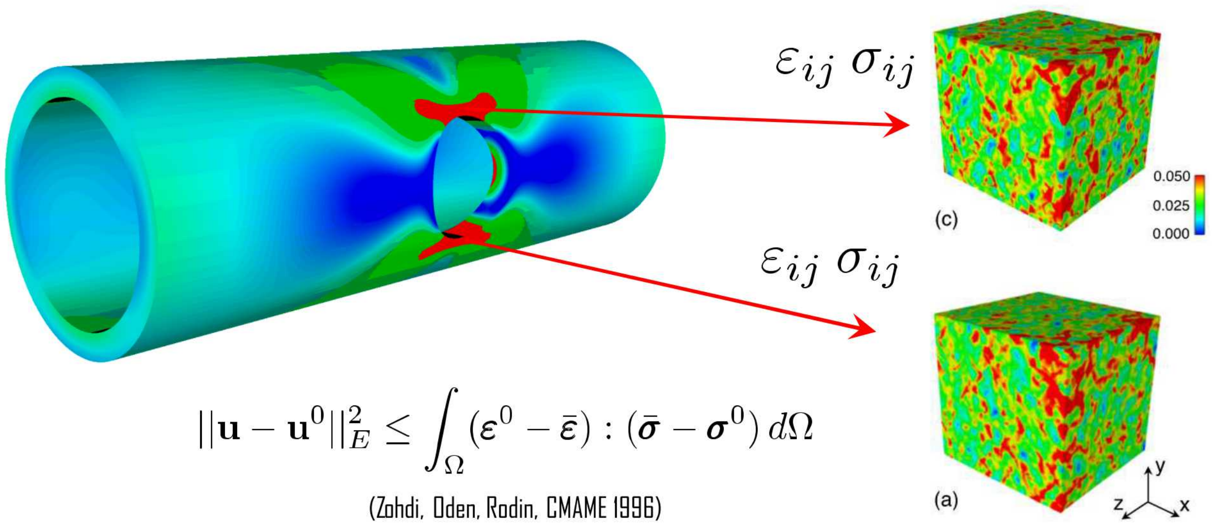

$$||\mathbf{u}-\mathbf{u}^0||_E^2 \leq \int_\Omega (\boldsymbol{\varepsilon}^0-\bar{\boldsymbol{\varepsilon}}) : (\bar{\boldsymbol{\sigma}}-\boldsymbol{\sigma}^0)\, d\Omega$$

(Zohdi, Oden, Rodin, CMAME 1996)

4. Compare to Direct Numerical Simulations of Full KMC Microstructure

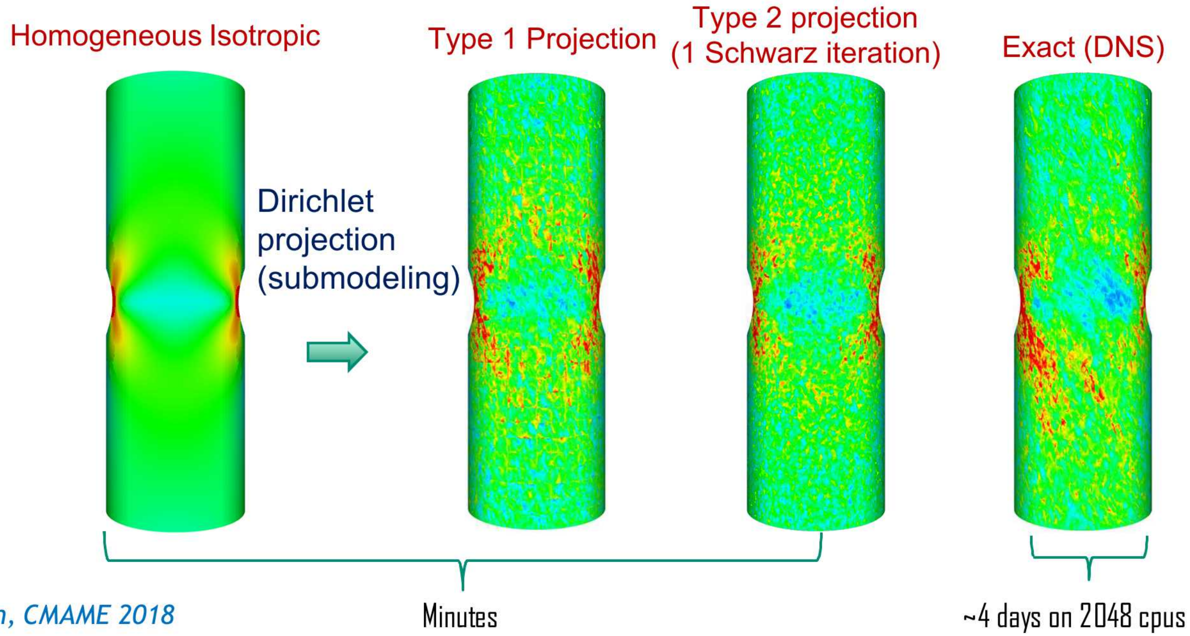

Bishop and Brown, CMAME 2018

Current State

- Can accurately predict residual stress in complex parts
    - Reduced order methods are faster than real-time
- Microstructure morphology predictions qualitatively match experiments
    - Orientation prediction has been demonstrated
- Part performance and failure can be predicted using existing tools
    - Part geometry can be used as a tool for flaw tolerance

Future Directions

- More efficient thermo-mechanical process simulations (analytical heat sources, FFT, etc.)
- Process-aware design optimization considering residual stress (current PLATO LDRD)
- Orientation and porosity prediction in SPPARKS
- Microstructure optimization for locally-tailored properties
- Rapid part acceptance/rejection based using Deep Learning

Backup Slides

Modeling the Effect of Pores and Surface Roughness From CT Scan in Follow-up Investigation

Clean STL in MeshLab

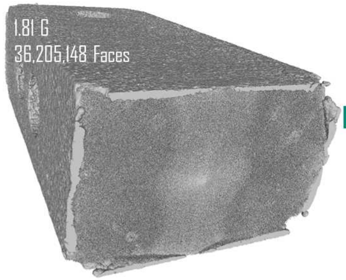

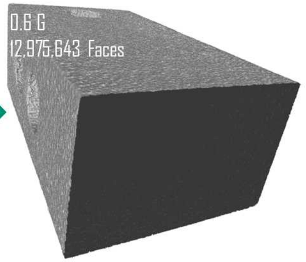

Modify in STL in Blender

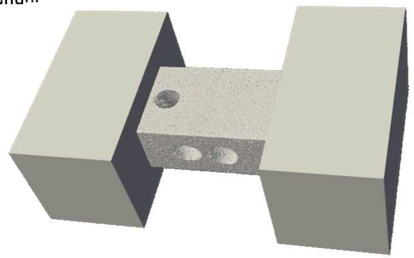

Mesh defeatured geometry in Cubit

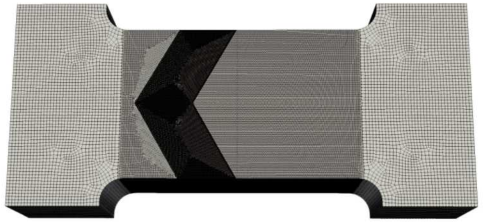

Cut with STL file using Sculpt

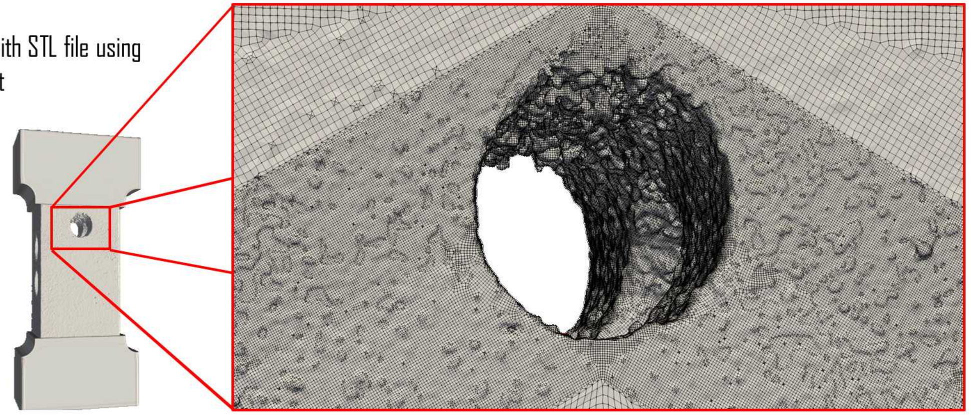

Generate pore SPN file using Python, Create STL file with Sculpt and Cubit, and clean up voids file using MeshLab

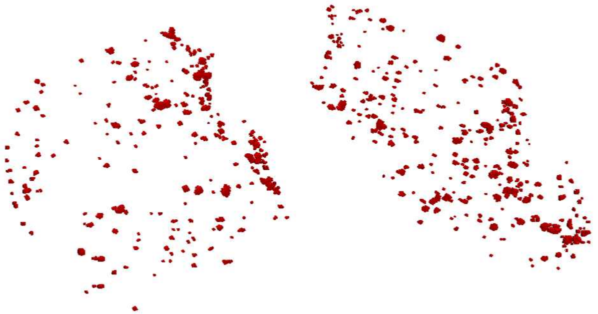

ve voids of interest from mesh
Sculpt

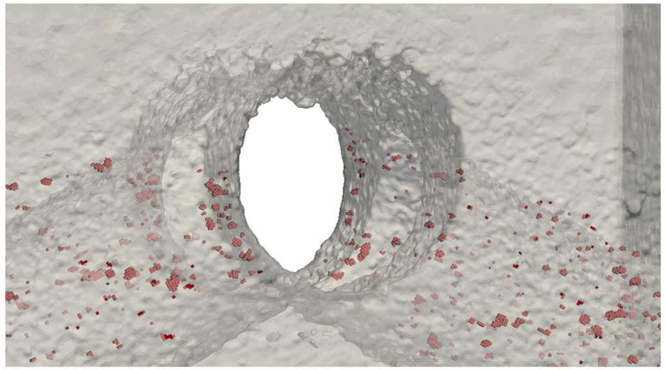

Slide Courtesy: Kyle Karlson

SPPARKS Direct Coupling With Finite Difference Thermal Conduction Model

- 2.8 x 2.8 x 5.5 mm domain
- Process parameters calibrated for 3D Systems ProX DMP 200 machine
  - Layer thickness = 30 μm
  - Hatch spacing 50 μm
  - Scan rate = 1400 mm/s
  - Laser power = 129 W
  - Scan strategy = +/-90 alternating
- Includes powder phase with 0.01 of solid conductivity
- Simulation domain boundaries fixed at 300K
- 5 μm grid
- 21.8 m of scan path simulated
- 157 layers

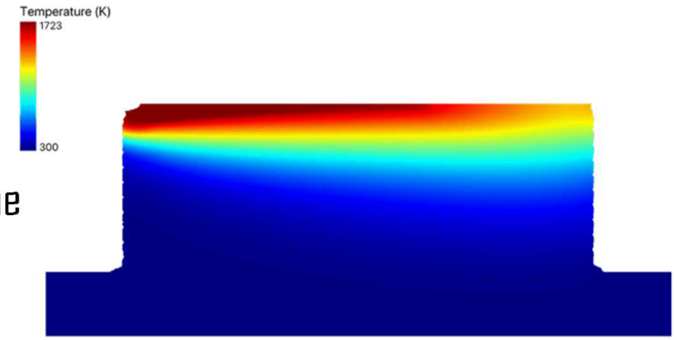

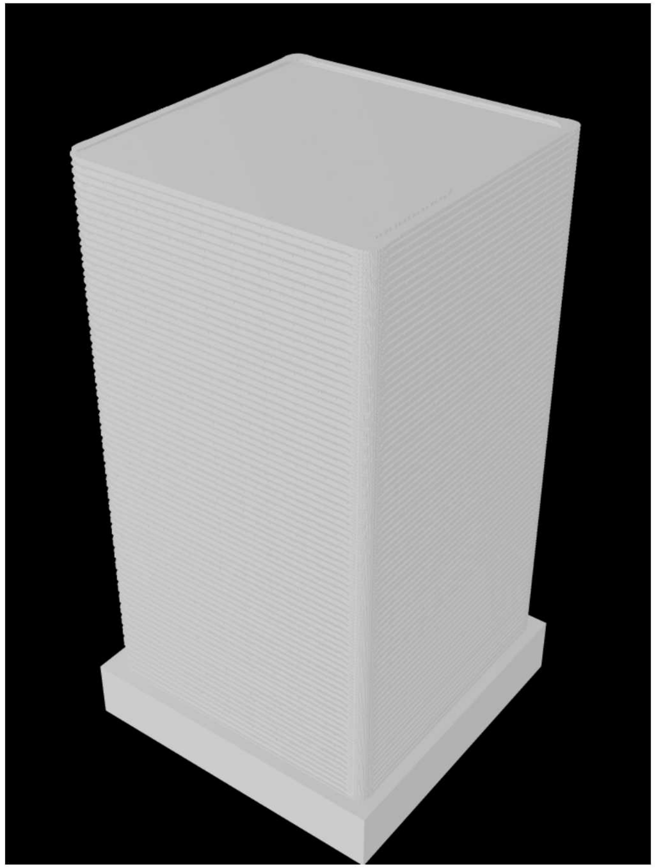

Theron Rodgers

Microstructure Evolution is Sensitive to Thermal Parameters

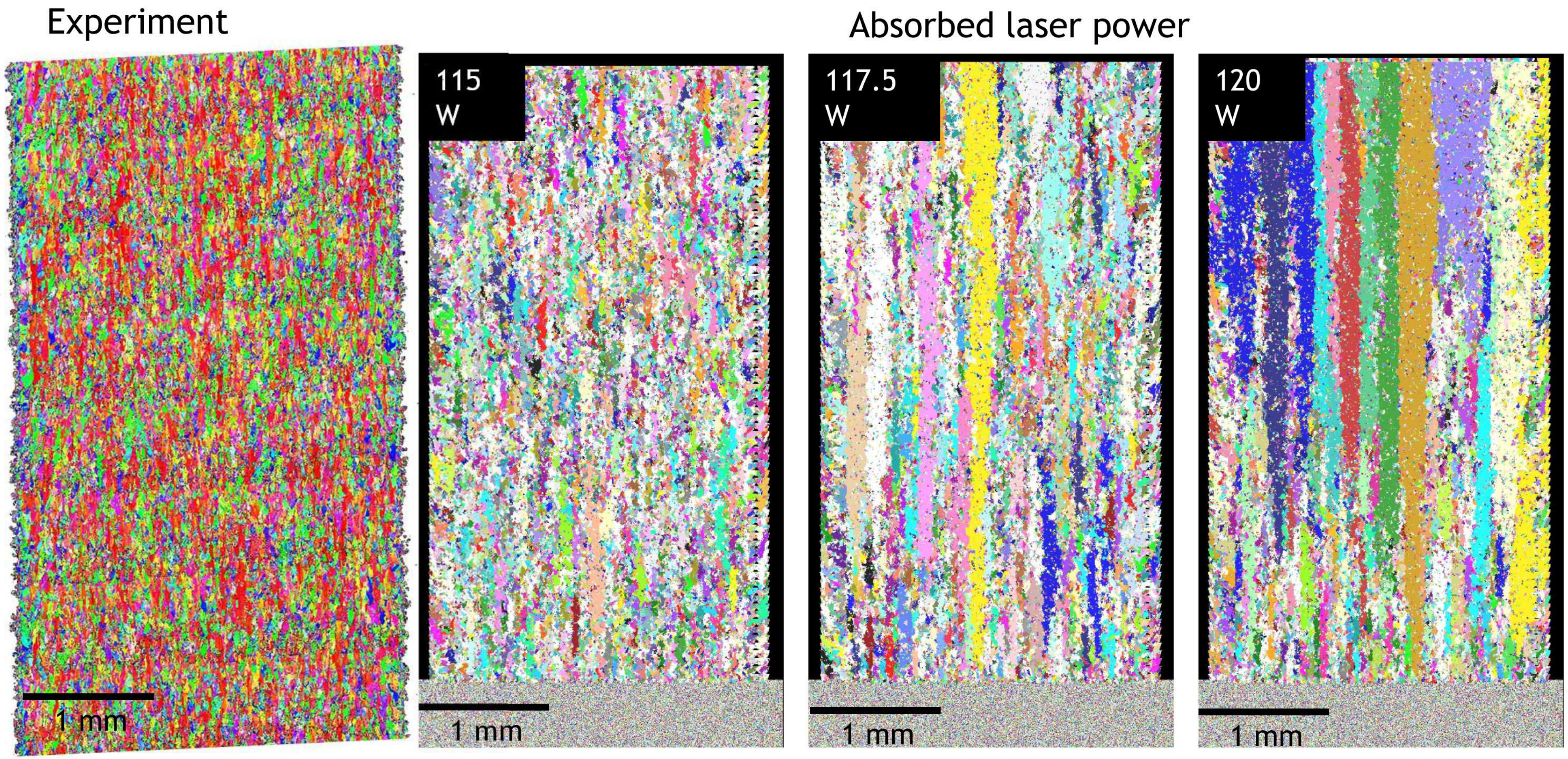

All simulations performed with nucleation densities of 8e13

Top View of Build

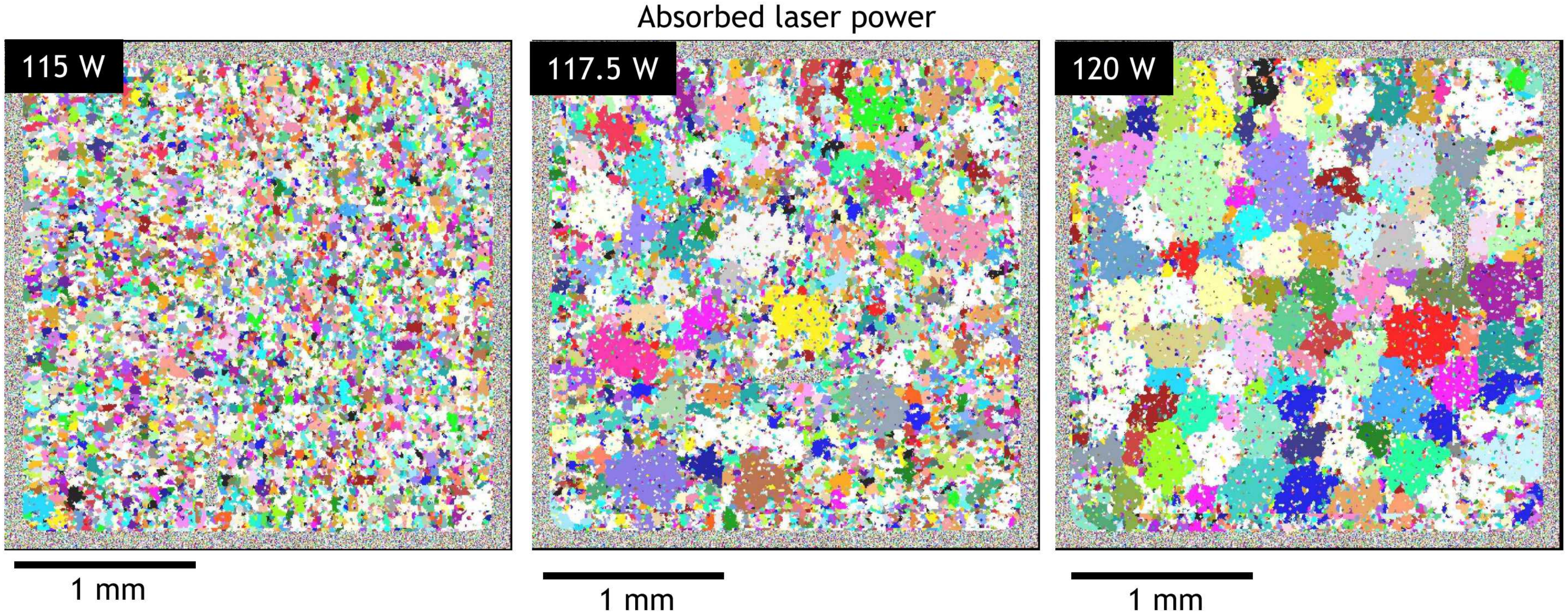

G/R and Grain Size Plots

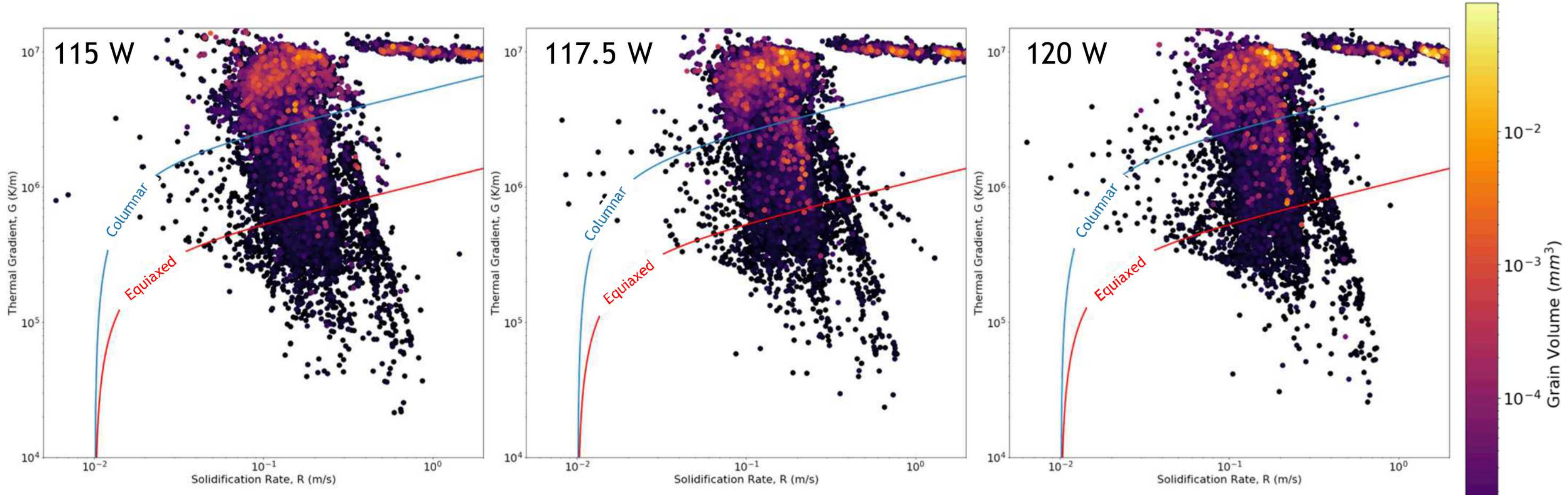

- Maximum grain size increases significantly with power
- Increasing power results in subtle shift upwards into mixed/columnar regime
- Maps do not provide significant information about degree of remelting -> resulting in similar distributions but orders-of-magnitude variations in grain size
- Each dot represents an individual grain (small grains over-represented vs volume fraction)
- G&R values recorded at grain centroid; may not represent entire grain

Theron Rodgers

Up-close comparison

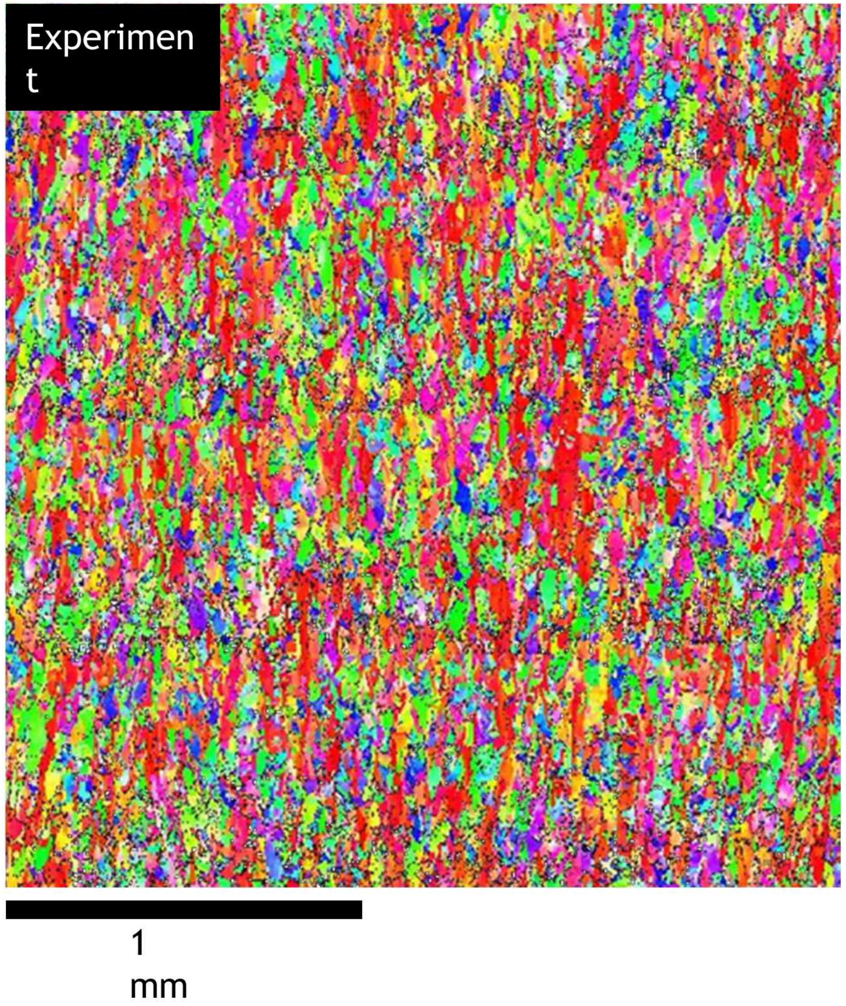

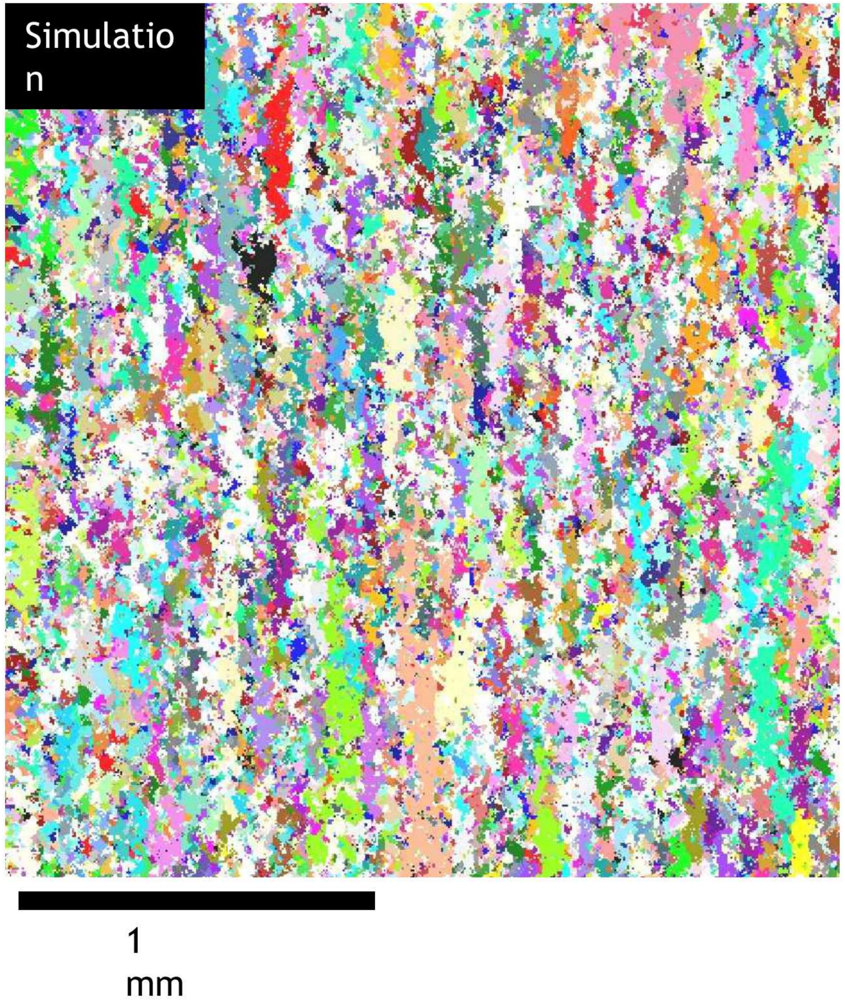

Theron Rodgers

How do we account for unknown critical flaw such as tunneling porosity? High Throughput Characterization + UQ?

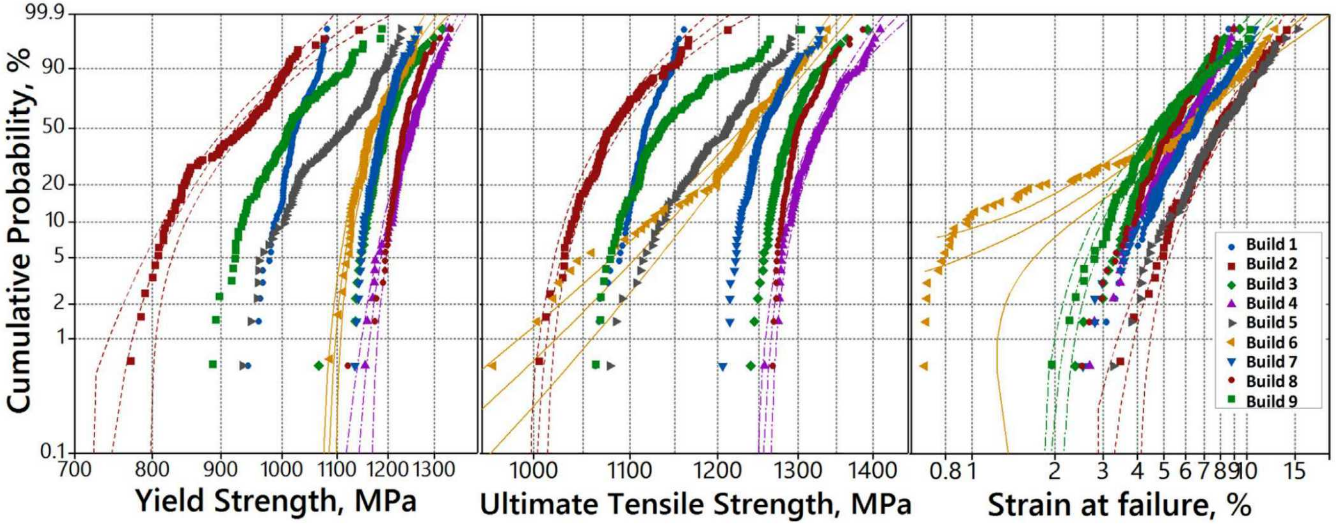

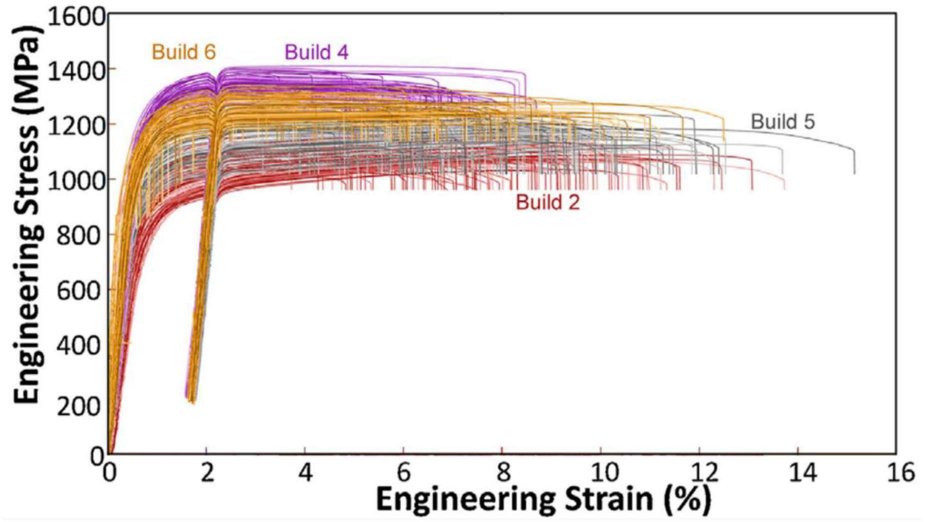

Variation from Different Builds of Same Part from Same External Vendor

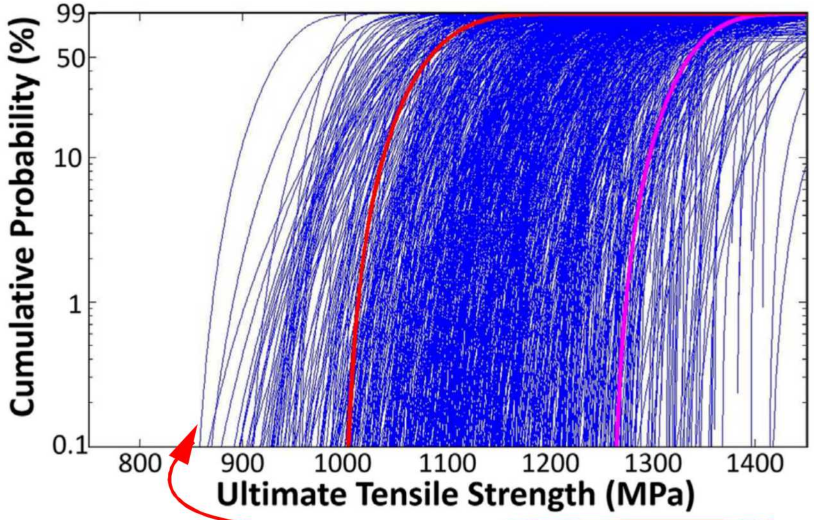

Cumulative Probability Distributions created by sampling Weibull parameters from multi-variate Gaussian distribution – Could provide lower bound on performance

Boyce et al., Advanced Engineering Materials 2017

Microstructure By Design

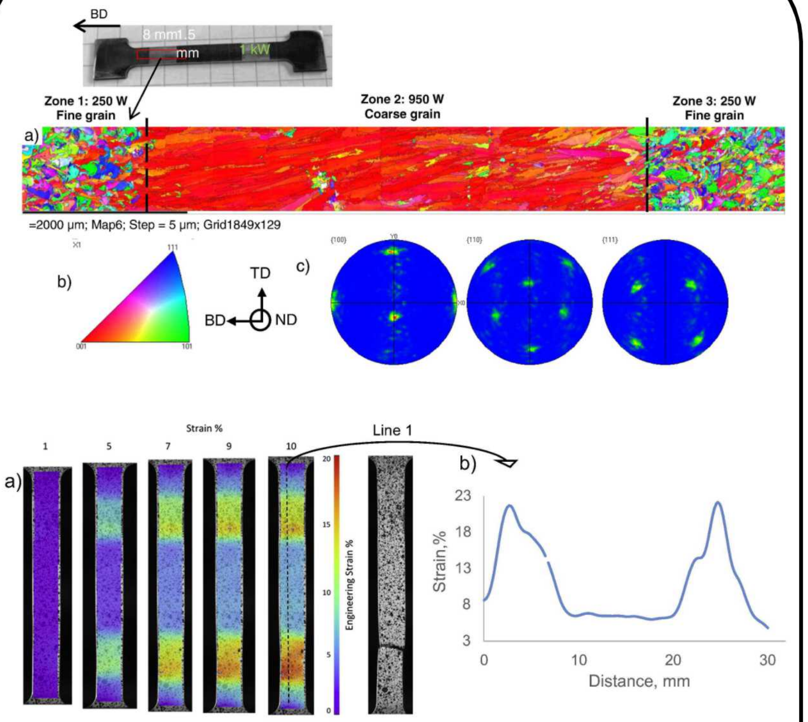

Process-dependent Microstructure (Popovich *et al.*, Materials & Design, 2017)

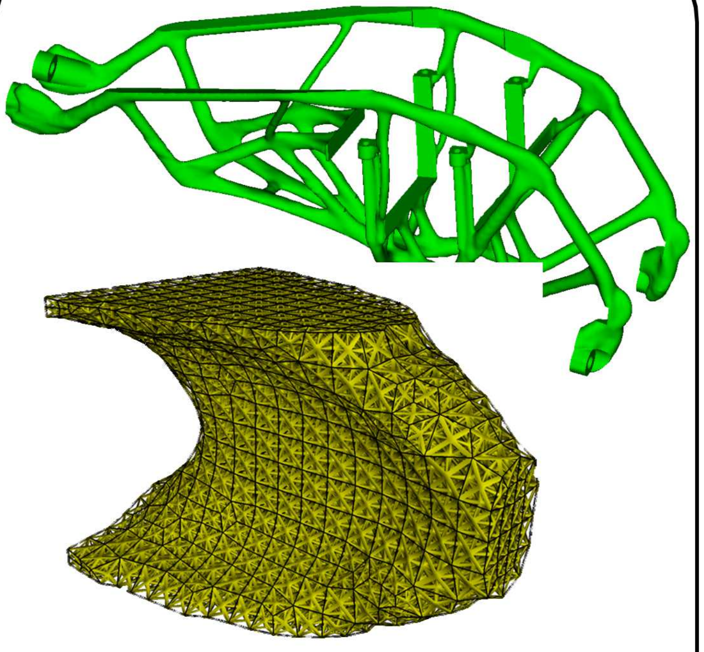

Design Optimization Code Such as PLATO

Site-specific optimized microstructure through process control

Jared et al., Scripta Materialia 2017

Microstructure Prediction in **S**tochastic **P**arallel **PAR**ticle **K**inetic **S**imulator (SPPARKS)

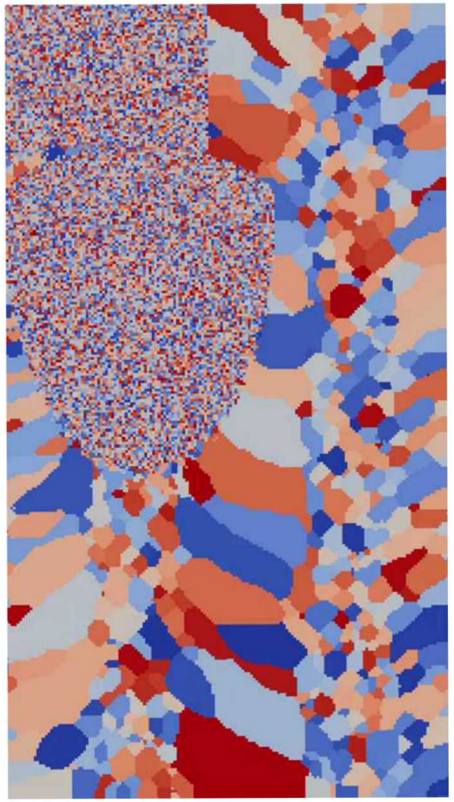

kMC & Solidification Structure

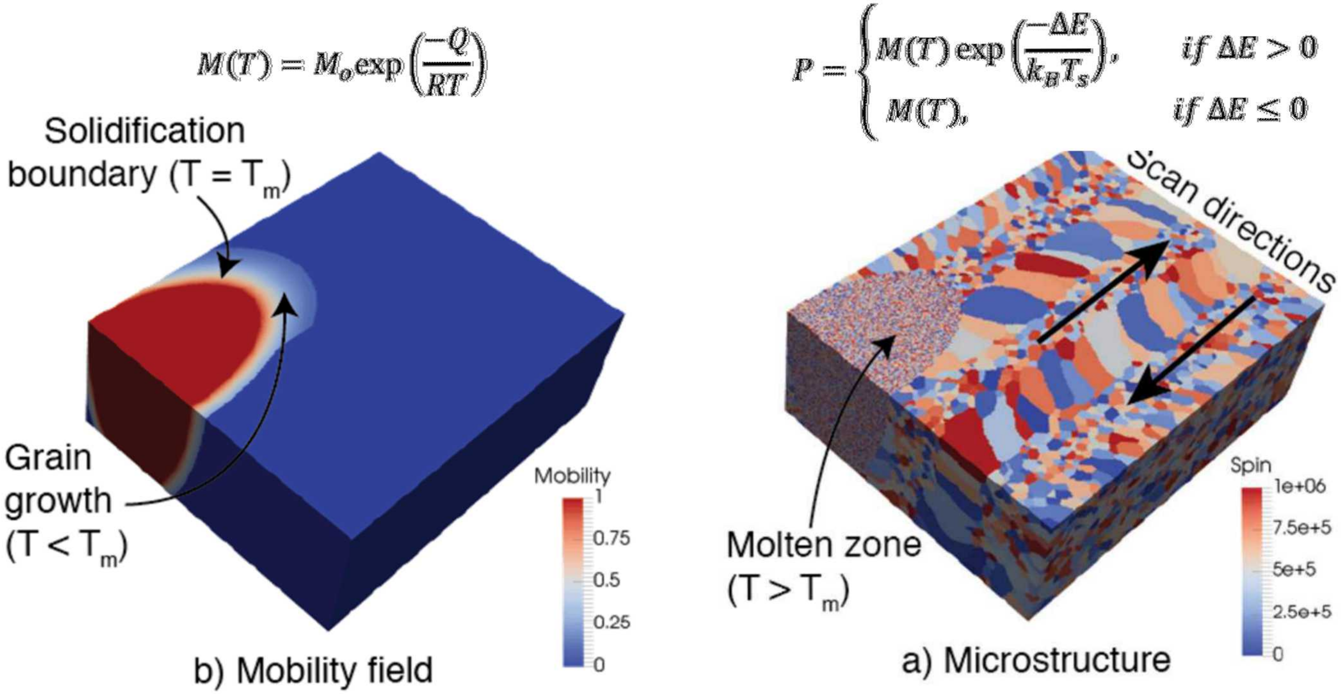

- The molten zone randomizes grain identities when it enters a region.
- Along the trailing surface, voxels either join existing columnar grains or form new grains.
- The temperature gradient creates a corresponding gradient of grain boundary mobilities via an Arrhenius relationship.

Transition From Equiaxed to Columnar Structure Predicted, Though Grain Size Was Too Large

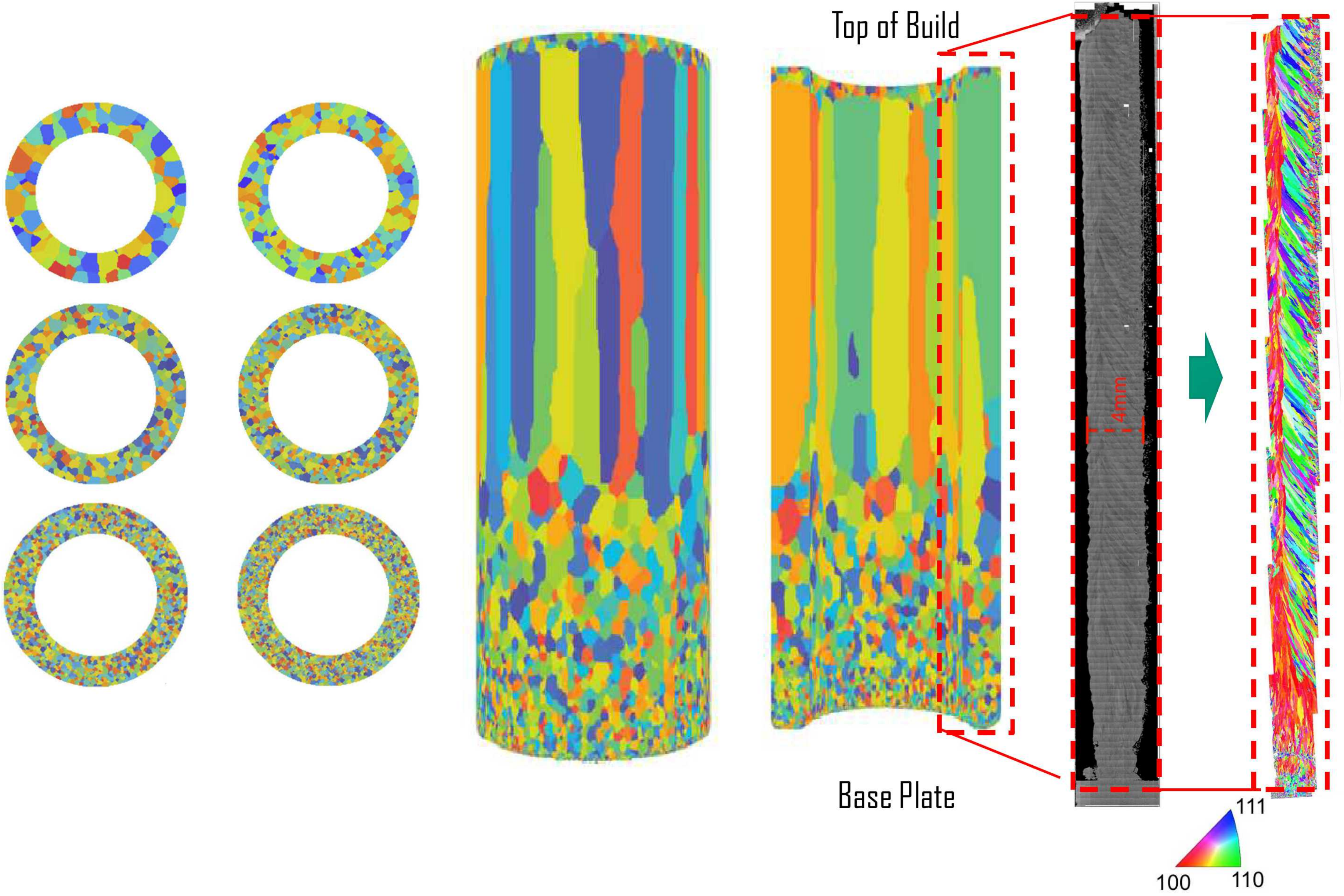

Johnson *et al.*, *Computational Mechanics 2018*